

Thick Arnold tongues*

Mark Levi and Alexey Okunev

November 4, 2024

Abstract

We introduce and study a physically motivated problem that exhibits interesting and perhaps unexpected mathematical features. A cellular flow is a two-dimensional Hamiltonian flow of the Hamiltonian $H(x, y) = \cos(x) \cos(y)$. We study a simple model of the dynamics of an inertial particle carried by such a flow, subject to viscous drag and to an additional constant external force (b, a) . In the limiting case of zero inertia particles the dynamics is Hamiltonian with $H(x, y) = \cos(x) \cos(y) - ax + by$. For small but nonzero a, b there appear “channels” of trajectories that wind their way to infinity, of small relative measure, while most trajectories remain periodic.

By contrast, for nonzero inertia, no matter how small, almost all particle trajectories drift to infinity. Moreover, the asymptotic direction of this drift no longer coincides with the direction of forcing, and rather becomes Cantor-like function of the forcing direction a/b , and with an unexpected feature: the plateaus of this function occupy a set of full measure. Moreover, the complement to this set has zero Hausdorff dimension. In a two-parameter representation (one parameter being the forcing direction a/b , the other the drag coefficient), this gives rise to Arnold tongues, the tongues corresponding to rational slopes of drift. However, unlike Arnold’s example, the complement to the union of all tongues has zero measure. This is explained by the behavior of rotation number for monotone families of circle maps with flat spots.

1 Introduction and Results

1.1 Background

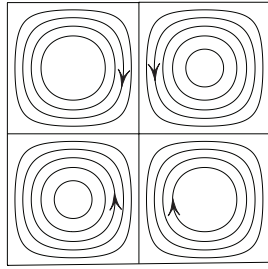
The problem of particle transport by fluid flow has been studied extensively - in experiment, theory and computation. The case of spherical particles in Newtonian fluids has been modeled by the so-called Maxey–Riley equation ([1]), which is Newton’s second law for the particle accounting for buoyancy, drag, inertial effect of the fluid (added mass), and boundary layer (memory) ([2, 3] and references therein). Many authors consider a simplified form of this equation, where the only force coming from the fluid is the drag proportional to the velocity mismatch between the particle and surrounding fluid:

$$\ddot{\mathbf{x}} = -\frac{1}{\varepsilon}(\dot{\mathbf{x}} - \mathbf{v}(\mathbf{x})), \quad (\mathbf{x}, \dot{\mathbf{x}}) \in \mathbb{R}^4. \quad (1.1)$$

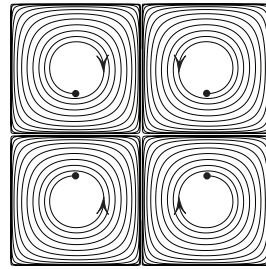
Here, $\mathbf{x}(t) \in \mathbb{R}^2$ is the particle position, $\mathbf{v}(\mathbf{x})$ is the fluid velocity at \mathbf{x} , and $\varepsilon = m/k$, where m is the particle mass and k is the drag coefficient (see Appendix A for details). The smaller ε , the smaller the impact particle’s inertia has on the dynamics. When $\varepsilon = 0$ (zero-inertia case) the particle just moves together with the surrounding fluid: $\dot{\mathbf{x}} = \mathbf{v}(\mathbf{x})$; we will discuss what happens when ε is small but positive.

Many studies on particle transport deal with the particular case when fluid motion is given by the cellular flow (also called the 2-D Taylor-Green vortex flow), i.e., the Hamiltonian flow along the contour lines of $H = \cos x \cos y$, Figure 1a. Cellular flow is often used to model particles (e.g., plankton or microplastic) carried by convective motions near sea surface ([4, 5, 6]) or as a very simplified model of turbulence ([7]). The dynamics of (1.1) with \mathbf{v} being a cellular flow is quite simple, as Figure 1b illustrates: the particles approach the cell boundaries. Additional effects can make the problem quite nontrivial, and there is a vast literature on the subject. This includes studying the dynamics of particles influenced by random thermal noise ([8, 9, 10, 11]), the roles of particle shapes, (asymmetric [12],

*ML acknowledges partial support by the NSF grant DMS-9704554



(a) A cellular area-preserving flow in \mathbb{R}^2 given by the Hamiltonian $H(x, y) = \cos x \cos y$



(b) Trajectories of particles carried by (1.1) where \mathbf{v} is an in Figure 1a and $\varepsilon = 1/25$.

Figure 1: A particle in a cellular flow

compound [13], self-propelled [14, 15]), particles driven by a magnetic force ([16]), particles in a time-dependent cellular flow ([17, 18, 19]). The list above is by no means exhaustive; additional references can be found in the cited papers.

The case of particles in the cellular flow subject to a constant external force (gravity) was considered as early as 1949 by Stommel [20], who considered the zero-inertia case. The positive inertia case was considered by Maxey and Corrsin in [7] for aerosol particles (i.e., particles with the density much greater than that of the fluid). They carried out a numerical investigation of this problem for a wide range of parameters and noticed two surprising effects. First, cellular flow makes particles settle much faster than in the still fluid. Second, particles equidistributed initially tend to concentrate on certain curves. The case of aerosol particles was then rigorously investigated in [21] for a special case when the gravity direction is aligned with the flow cells orientation, and particle concentration was proved. In [22], the case of arbitrary particle density was considered. Curiously, when the particle and fluid density are of the same order, chaotic dynamics was observed even without the external forcing [23]. These results are nicely summarized in the review [24, §3].

Mathematically, accounting for a constant external force acting on an aerosol particle (as in [7, 21]) can be reduced to adding a constant term to the fluid velocity, i.e. to taking $\mathbf{v}(\mathbf{x}) = \mathbf{u}(\mathbf{x}) + \mathbf{w}$ in (1.1), where $\mathbf{u}(\mathbf{x})$ is the fluid velocity, and \mathbf{w} is the terminal velocity of a particle pulled by gravity in a still liquid. This reduction is explained in [7], it is also summarized in Appendix A. One can write the resulting $\mathbf{v}(\mathbf{x})$ as a Hamiltonian vector field by adding a linear part to the Hamiltonian giving the fluid motion (\mathbf{u} must be Hamiltonian if the fluid is incompressible). If $\mathbf{w} = (b, a)$, we get

$$\mathbf{v} = \left(\frac{\partial H}{\partial y}, -\frac{\partial H}{\partial x} \right), \quad \text{with } H(x, y) = \cos x \cos y - ax + by. \quad (1.2)$$

The dynamics of the resulting vector field $\dot{\mathbf{x}} = \mathbf{v}(\mathbf{x})$ is referred to as zero-inertia case ([7]), it results from the assumption that the particle's relative velocity in the fluid equals the terminal velocity \mathbf{w} so that gravity is compensated by the fluid drag.

1.2 Subject of this paper

We give a rigorous analysis of the model (1.1) with \mathbf{v} given by (1.2) focusing on the direction of particle drift. Note that one can also consider Hamiltonians with the periodic part other than $\cos x \cos y$ in (1.2) using similar methods. As an example, Figure 2 shows trajectories of (1.1) where $\cos x \cos y$ in (1.2) has been replaced by a Hamiltonian with a 3-fold symmetry.¹Let us consider first the “unperturbed” case of $\varepsilon = 0$, corresponding to

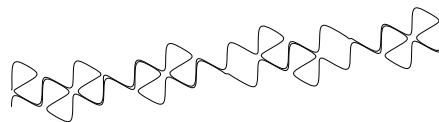


Figure 2: Two trajectories of (1.1) where \mathbf{v} has a 3-fold symmetry. The trajectories are separated by stable manifolds of equilibrium points.

the Hamiltonian vector field (1.2). Trajectories are the level curves of H . For the periodic case of $a = b = 0$ shown in Figure 1a the picture is trivial; but case of nonzero a, b , illustrated in Figure 6 in Section 2, is already quite interesting combinatorially.

Changing (a, b) from zero gives rise to “channels” consisting of unbounded trajectories winding their way to infinity between homoclinic cells (Figure 6 in Section 2). These trajectories have interesting combinatorics related to continued fraction expansion of the slope b/a . This problem has been studied in [25, 26, 27, 28] in a somewhat more general setting.

The dynamics changes drastically for $\varepsilon > 0$. Figure 3 shows typical trajectories of (1.1) for small ε ; in all numerical simulations these trajectories drift in a rational direction regardless of the direction of imposed forcing. Moreover, the drift slope m can be sensitive to the slope $\alpha = a/b$ of imposed forcing (compare the two top cases in Figure 3: half a degree change in forcing direction causes a drastic change of the trajectory). This figure, as well as other numerical experiments, may give a false impression of discontinuous dependence of the drift slope m on the slope α of imposed forcing.

Actually, we will later see that $m(\alpha)$ is continuous; the false impression of discontinuity is explained by the fact that m is a Cantor-like function that is locally constant on a full measure set. Thus the slope of trajectories changes on the set of slopes $\alpha = a/b$ of zero measure (Figure 4a below), giving the impression of discontinuity.

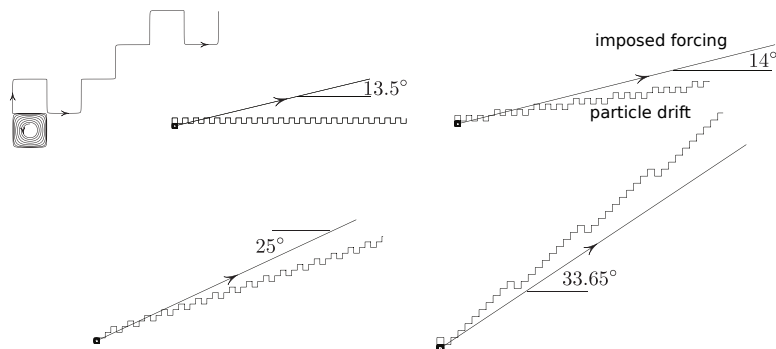


Figure 3: Trajectories of the system (1.1), (1.2) with $\sqrt{a^2 + b^2} = 0.02$ and $\varepsilon = 1/25$.

1.3 Main results

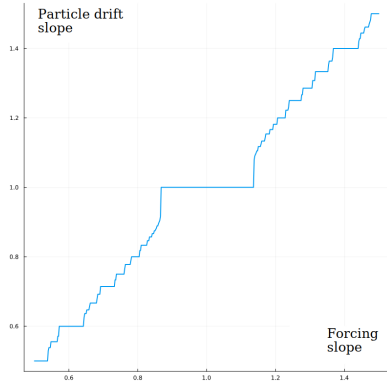
Consider the system (1.1) with the vector field \mathbf{v} given by (1.2). This is a model of a particle carried by the cellular flow and pulled by a constant forcing (b, a) such as gravity proposed by Maxey and Corrsin [7]. Our main result describes the dependence of the asymptotic slope m of particles’ forward trajectories on the forcing slope $\alpha = \frac{a}{b}$.

For definiteness, we assume that b and ε are fixed, so that a is tied to α via $a = \alpha b$. Also, a and b will be non-zero and sufficiently small but fixed, but ε is much smaller, as is stated in the theorem below. By symmetry, it suffices to consider the case $b \geq a > 0$. We relax the condition $b \geq a$ to $a \leq 1.5b$ to allow the forcing slope $\frac{a}{b}$ to pass through 1.

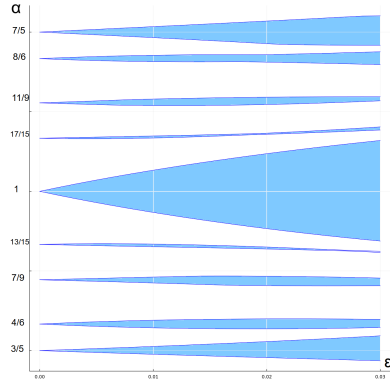
Theorem 1.1. *There exists $\gamma > 0$ such that for any positive $\delta < \gamma$ there exists $\varepsilon_0 > 0$ such that, provided that a and $b \in [\delta, \gamma]$ with $a \leq 1.5b$ and $\varepsilon \in (0, \varepsilon_0)$, the following holds for (1.1) with \mathbf{v} given by (1.2).*

1. *For all initial data $(\mathbf{x}_0, \dot{\mathbf{x}}_0) \in \mathbb{R}^4$ with the exception of a countable union of codimension one hypersurfaces the particle’s forward trajectory $\mathbf{x}(t)$ in \mathbb{R}^2 is unbounded and follows some ray at a finite distance. Moreover, the slope m of this ray is the same for all such initial data. We will call this m the drift slope.*

¹We took $H(x, y) = h(\mathbf{x})h(R\mathbf{x})h(R^2\mathbf{x}) - ax + by$ with $\mathbf{x} = (x, y)$, $h(\mathbf{x}) = \sin x \sin y$ and with R being the rotation around the origin by $2\pi/3$.



(a) Cantor-like dependence of the particle drift slope on the direction of external force. Particle's drift direction is rational for Lebesgue-almost all directions of external force.



(b) Arnold tongues [29], i.e., parameter values corresponding to a fixed rational particle drift slope, shown in blue. If all the tongues were shaded, they would occupy full measure.

Figure 4: Particle drift direction

2. The drift slope m has a Cantor-like dependence on the direction $\alpha = \frac{a}{b}$ of the forcing (Figure 4a). To be precise, we fix $b \in [\delta, \gamma]$, $\varepsilon \in (0, \varepsilon_0)$ and set $a(\alpha) = \alpha b$, $I = [\delta/b, \min(\gamma/b, 1.5)]$. Then $m(\alpha)$, $\alpha \in I$ is a Cantor-like function: it is continuous, non-decreasing, and the set $C \subset I$ of points where m is not locally constant is a nowhere dense perfect set. Also, $C = \{\alpha \in I : m(\alpha) \notin \mathbb{Q}\}$, and each rational value $m(\alpha) = p/q$ achieved on I is achieved on a closed nondegenerate interval (plateau) $m^{-1}(p/q)$.
3. The set C has zero Hausdorff dimension (and hence also zero Lebesgue measure). According to this and the previous item, $m(\alpha)$ is rational for almost all values of the parameter α .
4. The function $m(\alpha)$ is "steep to all orders" at the endpoints of each plateau $m^{-1}(p/q)$, Figure 5. More precisely, let α_0 be the right endpoint of a plateau and let $\Delta m = m(\alpha_0 + \Delta\alpha) - m(\alpha_0)$. Then, there exist $c > 0$ and $\delta > 0$ such that $\Delta\alpha < e^{-\frac{c}{\Delta m}}$ when $\Delta\alpha \in (0, \delta)$. A similar statement holds for the left endpoint of every plateau.

Note that this inequality implies that for any $n \in \mathbb{N}$ we have $(\Delta m)^n \gg \Delta\alpha$ when $\Delta\alpha \rightarrow 0^+$ – that is, the graph of $m(\alpha)$ is tangent to all orders to vertical lines passing through the plateau's endpoints.

Particle drift slope $m(\alpha)$ can be described in terms of the rotation number of a family of circle maps, see Section 1.4 below. It is a classical fact that rotation number of a typical monotone one-parameter family of circle diffeomorphisms is a Cantor-like function with a plateau at each rational value; a model example is the Arnold family [29] $x \mapsto x + \alpha + \varepsilon \sin x$. However, $m(\alpha)$ being rational on a full measure set of parameters is in marked contrast with the Arnold family, where the rotation number is believed to be irrational on a set of positive measure for small ε , [30]. This property was observed for Cherry flows on the 2-torus [31]. An interesting feature of our setting is that while for $\varepsilon = 0$ the measure of the set of

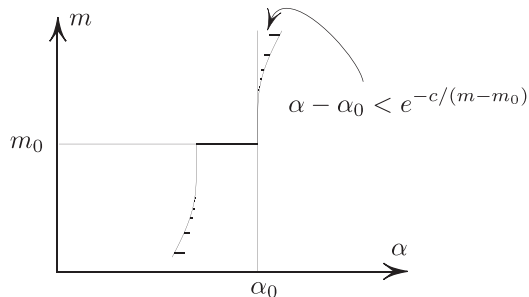


Figure 5: Steepness of $m(\alpha)$ near the ends of plateaus.

α with $m(\alpha)$ irrational is full, this measure collapses to zero as soon as $\varepsilon > 0$, no matter how small. That is, the blue tongues in Figure 4b occupy full measure (as Theorem 1.1 states), justifying the term "thick Arnold tongues".

It should be noted that even the unperturbed ($\varepsilon = 0$) dynamics, that of the basic Hamiltonian system with the periodic+linear Hamiltonian (1.2), is surprisingly nontrivial. As a side result of this article we describe the combinatorics of unbounded trajectories of this system, relating it to number-theoretic properties of a/b in Section 2 below. We should note that this reduced problem is a special case of a well-known problem studied by Arnold, Dynnikov, Novikov, Zorich and others ([25, 26, 27, 28] and references therein): to describe the foliation of a closed surface given by a closed 1-form. In our case, the surface is the torus $\mathbb{R}^2/2\pi\mathbb{Z}^2$, and the 1-form is dH .

1.4 Monotone families of circle maps with flat spots

In this section we briefly explain the underlying dynamical mechanism behind the behavior of the particle drift slope described in Theorem 1.1.

The particle dynamics given by (1.1) and (1.2) can be reduced to a continuous circle map that is constant on two intervals and is monotone increasing elsewhere. This reduction is done in Section 3. Briefly, the flow of (1.1) in \mathbb{R}^4 has a globally attracting two-dimensional normally hyperbolic invariant manifold. This manifold inherits the periodicity of \mathbf{v} in \mathbf{x} so that the problem reduces to the flow on a 2-torus. This flow admits a transversal circle, and the resulting Poincaré map of the circle captures the entire dynamics of (1.1) in \mathbb{R}^4 .

This first return map turns out to be monotone increasing and continuous apart from two jump discontinuities, as explained later in Section 3.2 (Figure 9). In particular, the particle drift slope is the rotation number of the circle map (up to a linear transformation). So the dependence of the drift slope on the forcing slope is captured by the dependence of the rotation number on the parameter in a one-parameter family of circle maps. For convenience we will consider the family of inverse maps extended to the jump intervals as a constant, i.e. a family of continuous degree one circle maps with flat spots. The properties of this family are captured by the definition below. Very similar² families naturally occur in the study of Cherry flows on torus and of truncations of non-invertible circle endomorphisms. They were studied by Boyd, Boyland, Graczyk, Palmisano, Świątek, Veerman, and others ([31, 32, 33, 34, 35, 36] and references therein).

Definition 1.2 (Monotone family of circle maps with flat spots). *Let f_s be a one-parameter family of circle maps $f_s : S^1 \mapsto S^1$, where $S^1 = \mathbb{R}/\mathbb{Z}$ defined for $s \in [s_{min}, s_{max}]$ and continuous with respect to both x and s . Let $\tilde{f}_s : \mathbb{R} \mapsto \mathbb{R}$ be a lift of f_s . We will say that f_s is a monotone family, if*

1. $\tilde{f}_s(x)$ is continuous and non-decreasing with respect to both x and s .
2. f_s has degree 1 for all s .
3. There are m flat spots for each s , where $m \geq 1$ is an integer independent of s . More precisely, there exists $m \geq 1$ and m disjoint closed arcs $I_j(s)$ such that $f_s|_{I_j}$ is constant. The endpoints of these arcs depend on s continuously.
4. There exists $\lambda > 1$ such that for each s the map f_s is λ -expanding outside $\cup_{j=1}^m I_j$: $\tilde{f}_s(x)$ is differentiable in x and $\frac{d}{dx}\tilde{f}_s(x) > \lambda$.
5. Pick any lifts \tilde{I}_j , $j = 1, \dots, m$ of the flat spots and let $\tilde{b}_j(s) = \tilde{f}_s(\tilde{I}_j(s))$ be the "height" of the plateau above \tilde{I}_j . Then, each of these heights is differentiable with respect to s and increases with the speed separated from zero: there exists $\nu > 0$ such that $\frac{d}{ds}\tilde{b}_j(s) > \nu$ for all s , $j = 1, \dots, m$.

²Up to some differences such as that expansivity condition can be removed, certain conditions on the derivative near the flat spot (such as having bounded variation) can be required, and often the case of just one flat spot is considered.

The same argument as for circle homeomorphisms shows that such maps have a rotation number $\rho(s)$ which is also continuous and monotone in the parameter s , and the rotation number is rational if and only if there is a periodic orbit. Moreover, one can show that the rotation number is rational if and only if the image of the flat spot intersects itself, so a rational rotation number corresponds to a whole interval of the values of the parameter s . Hence, the graph of $\rho(s)$ is a Cantor-like function increasing when ρ is irrational and with plateaus at rational values of ρ . This is also common for circle homeomorphisms, e.g. for the Arnold family $f_s(x) = x + s + \varepsilon \sin x$, $\varepsilon \in (0, 1)$. A remarkable contrast with the case of homeomorphisms is that for maps with flat spots the set of the values of s with irrational rotation number has zero Lebesgue measure and, moreover, zero Hausdorff dimension. This was first proved by Boyd for a special case of families of the form $f_s(x) = f_x + s$ and then for generic classes of families of maps with *one flat spots* by Świątek [32] and Veerman [33]. Veerman also remarked that this statement can be generalized for any number of flat spots. We do this by extensive use of the ideas from [33].³

Theorem 1.3. *Suppose f_s , $s \in [s_{min}, s_{max}]$ is a monotone family of circle maps with flat spots, and \tilde{f}_s is its lift to \mathbb{R} . Then*

1. *The rotation number*

$$\rho(s) = \lim_{n \rightarrow \infty} \frac{(\tilde{f}_s)^n(\tilde{x}) - \tilde{x}}{n}$$

*exists*⁴. *Moreover, $\rho(s)$ is continuous and non-decreasing.*

2. *For any $\frac{p}{q} \in \mathbb{Q}$, its preimage $\rho^{-1}(p/q)$ is a closed interval with positive length (unless it is an empty set). For any $r \notin \mathbb{Q}$, its preimage $\rho^{-1}(r)$ is a point (unless it is an empty set).*
3. *The set $C = \rho^{-1}([s_{min}, s_{max}] \setminus \mathbb{Q})$ is a nowhere dense perfect set.*
4. *The Hausdorff dimension $\dim_H(C) = 0$.*
5. *The function $\rho(s)$ is “steep to all orders” at the endpoints of each plateau $\rho^{-1}(p/q)$, as described in Theorem 1.1.*

This result explains the properties of $\rho(\alpha)$ claimed in Theorem 1.1. It is proved in Section 4 relying extensively on the ideas from [33].

2 The Hamiltonian flow

Before studying particle transport in the sections that follow, let us make some observations on trajectories of the Hamiltonian flow (1.2):

$$\dot{x} = -\cos x \sin y + b, \quad \dot{y} = \sin x \cos y + a. \quad (2.1)$$

For $a = b = 0$ the phase portrait is very simple, consisting of the square grid of separatrices (Figure 1a) with interiors of the squares filled by periodic orbits. Saddles form the lattice $(\frac{\pi}{2} + \pi k_1, \frac{\pi}{2} + \pi k_2)$, where $(k_1, k_2) \in \mathbb{Z}^2$.

³Instead of the expansivity (Property 4 in Definition 1.2) Veerman [33] requires that $\ln(\frac{d}{dx} f_s)$ has bounded variation outside the flat spot and uses this condition to prove a weaker form of expansivity. In the family originating from particle’s dynamics this variation is unbounded by Remark E.9 below, but expansivity holds, which motivates this difference compared to the setting in [33]. Also, this family has two flat spots, so we need to consider the case of more than one flat spot.

⁴That is, the limit exists and does not depend on the initial point $\tilde{x} \in \mathbb{R}$.

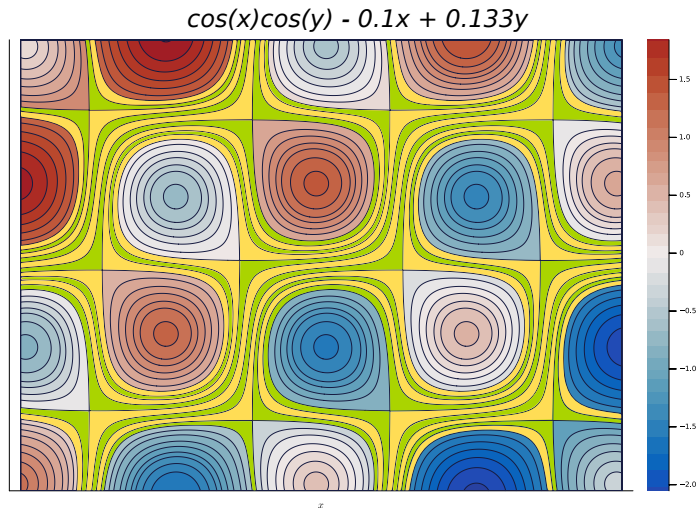


Figure 6: Level lines of the Hamiltonian (1.2). “Channels” are highlighted in yellow and green.

For $a, b > 0$ the phase portrait becomes somewhat nontrivial despite the simplicity of the Hamiltonian. For small a, b most of the phase space will still be filled by periodic trajectories bounded by homoclinic loops; however, certain “channels” appear, (Figure 6); these channels hug the original grid of the flow with $a = b = 0$, and all forward trajectories in these channels are now unbounded, with the exception of a zero measure set of those lying on stable manifolds of saddles. Any such unbounded trajectory stays within a bounded distance from the straight line $by - ax = 0$ (Figure 7a), since $by - ax = H - \cos x \cos y$, where H is constant along a trajectory, and $\cos x \cos y$ is bounded. So, the asymptotic direction of Hamiltonian trajectories is the same as the direction of the forcing vector (b, a) in (2.1). We shall see later that this is decidedly not the case for particles carried by the flow.

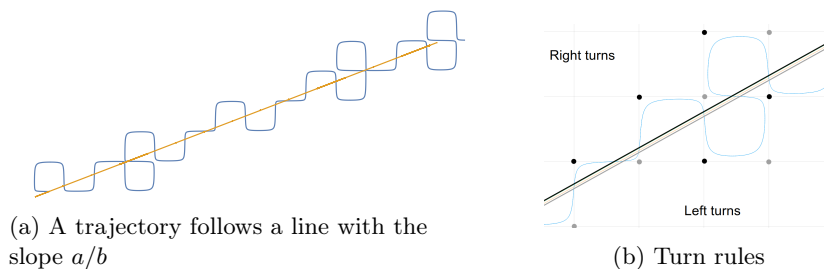


Figure 7: Fluid trajectories given by (2.1)

Combinatorics of Hamiltonian trajectories

A “chess” game. We now describe the combinatorics of unbounded Hamiltonian trajectories. This part is not used in the analysis of particle dynamics that leads to Theorem 1.1.

For small a and b , any unbounded trajectory is close to the net of separatrices of the unperturbed system with $a = b = 0$, (Figure 7a), and can be approximated by a broken path formed by abutting edges of the net. Every trajectory approaching a vertex makes a turn, either to the left or to the right depending on which side of the stable manifold the trajectory enters the saddle’s neighborhood (the trajectories we consider are unbounded and hence they do not lie on the stable manifolds of the saddles). The following “chess rule” gives a simplified combinatorial description of unbounded trajectories (such as one in Figure 7a). This description is valid for small a and b ; to be specific, we take $|a|, |b| < 0.1$.

Consider a chess coloring of the vertices of the square lattice $\{\frac{\pi}{2} + \pi\mathbb{Z}\}^2$ of the saddles of the Hamiltonian with $a = b = 0$. Namely, we call a vertex $(\frac{\pi}{2} + \pi k_1, \frac{\pi}{2} + \pi k_2)$ *odd* if $k_1 + k_2$ is odd and *even* otherwise. Also, consider two oriented parallel straight lines $by - ax = c_o$ and $by - ax = c_e$ ⁵ corresponding to odd and even vertices, respectively (Figure 7b). Assume that both lines do not pass through grid vertices (this is true if the considered trajectory is unbounded). Focusing our attention on the odd vertices first, the “odd” line divides these vertices into the left class and the right class; we label these odd vertices by L or R according to their class. Similarly, even vertices are divided by the “even” line into left and right classes, and again we label these by L or R accordingly. All vertices are now labeled, and we state *the path-generating rule*. Our path will consist of abutting horizontal and vertical edges connecting neighboring vertices. As we travel along an edge and meet a vertex, we turn right if the point is labeled R and turn left if the point is labeled L .

The idea behind this description is very simple: to understand if a right or a left turn happens at a vertex, one needs to compare the *constant* value of H along the trajectory with the value of H at the saddle of (2.1) near this vertex. The precise proof is given in Appendix B.

Area-preserving flows on surfaces and Novikov’s problem.

To put the Hamiltonian case in proper context, let us note that this is a particular case of the following much harder problem: study the foliation of a closed surface given by a closed 1-form.⁶ In our case, the surface is \mathbb{T}^2 and the 1-form is dH . For the torus case, Arnold [26] showed that, given that the periods of the 1-form are not commensurate, under a mild genericity condition there exists a transversal such that the corresponding first return map is conjugate to an irrational rotation by the angle equal to the ratio of the periods. As in our case, there might also be topological discs formed by closed finite leaves of the foliation (homoclinic loops). For higher genus surfaces, the foliation can be much more complicated; this is known as *chaotic regime*. This phenomenon was extensively studied by Dynnikov with several co-authors (cf. [37, 28] and references therein). For more background on this problem, we direct the reader to the survey by Zorich [27]. Another rich research area is mixing properties of area-preserving surface flows restricted to quasi-minimal components (such as the complement to the union of the interiors of homoclinic loops in our case, provided that a/b is irrational). An up-to-date discussion on this topic can be found in [38].

3 From particle dynamics to a circle map

3.1 Reduction to a torus flow

Two-dimensional attracting manifold. The simplified Maxey-Riley equation (1.1) is a singular perturbation of the flow $\dot{\mathbf{x}} = \mathbf{v}(\mathbf{x})$ in \mathbb{R}^2 . A general fact from singular perturbation theory commonly used in literature on particle transport (e.g., [39]) is that for small enough ε the flow given by (1.1) in \mathbb{R}^4 can be reduced to a small perturbation (of order ε) of the original flow in \mathbb{R}^2 : $\dot{\mathbf{x}} = \mathbf{v}(\mathbf{x}) + \varepsilon \mathbf{f}(\mathbf{x}, \varepsilon)$. This application of Fenichel’s results [40] on normal hyperbolicity is done by Rubin, Jones, and Maxey [21] (see also the book [41]) for cellular flow the case when gravity is aligned with cell orientation ($a = 0$), but can be done in the same way for any \mathbf{v} . To that end, let us rewrite (1.1) as a first order system:

$$\dot{\mathbf{x}} = \mathbf{y}, \quad \dot{\mathbf{y}} = -\frac{1}{\varepsilon}(\mathbf{y} - \mathbf{v}(\mathbf{x})), \quad (\mathbf{x}, \mathbf{y}) \in \mathbb{R}^4. \quad (3.1)$$

⁵The constants c_o and c_e depend on the value of H at the trajectory we are describing and are specified below in Appendix B.

⁶The following equivalent ([26], see also [27]) problem is known as Novikov’s problem on the semiclassical motion of an electron. Consider a level surface of some smooth function in the 3-torus \mathbb{T}^3 . Lift it to a periodic surface in \mathbb{R}^3 and intersect it by an arbitrary plane \mathbb{R}^2 . What can be said about the connected components of this intersection?

Applied to this problem, Fenichel's results imply the following proposition. We give just a quick sketch of the proof in Appendix C following the book [41] where a full proof can be found.

Proposition 3.1. *For any $M > 0$ there exists ε_0 such that for any a, b , and ε with $|a|, |b| < M$ and $|\varepsilon| < \varepsilon_0$:*

1. *The system (3.1), (1.2) has an invariant manifold \mathcal{M}_ε . It is globally attracting when $\varepsilon > 0$. For any $r \in \mathbb{N}$, \mathcal{M}_ε is $O(\varepsilon)$ -close in C^r to the manifold \mathcal{M}_0 given by $\mathbf{y} = \mathbf{v}(\mathbf{x})$.*
2. *The phase space \mathbb{R}^4 is foliated by stable fibers of the points of \mathcal{M}_ε . Those fibers are two-dimensional manifolds, they are C^r for any r , and for any point $q \in \mathbb{R}^4$ lying on the stable fiber of $p \in \mathcal{M}_\varepsilon$, its forward orbit exponentially converges to the orbit of p .*
3. *The dynamics on the invariant manifold \mathcal{M}_ε can be written using \mathbf{x} as a coordinate as*

$$\dot{\mathbf{x}} = \mathbf{v}(\mathbf{x}) + \varepsilon \mathbf{f}(\mathbf{x}, \varepsilon), \quad (3.2)$$

where $\mathbf{f} = \mathbf{f}(\mathbf{x}, a, b, \varepsilon)$ is C^r for any⁷ r and periodic in \mathbf{x} . Here $\mathbf{f}(\mathbf{x})$ is some non-Hamiltonian vector field with the leading terms given by $\mathbf{f} = -D\mathbf{v} \cdot \mathbf{v} + O(\varepsilon)$, where $D\mathbf{v}$ is the Jacobian matrix of $\mathbf{v}(\mathbf{x})$.

It should be noted that the leading term $-D\mathbf{v} \cdot \mathbf{v}$ of \mathbf{f} is negative convective derivative of \mathbf{v} , i.e. minus the acceleration of the trajectory of \mathbf{v} . If \mathbf{v} happens to be a Hamiltonian vector field (as in our case), then

$$\mathbf{f} = (H_{yy}H_x - H_{xy}H_y, H_{xx}H_y - H_{xy}H_x) + O(\varepsilon)$$

Curiously, the divergence of the negative of convective derivative of a Hamiltonian flow is twice the Hessian determinant of H :

$$\operatorname{div} \mathbf{f} = 2 \det H'' + O(\varepsilon).$$

Choice of a fundamental domain. The vector field $\mathbf{v}(x, y)$ given by the Hamiltonian (1.2) is 2π -periodic in both x and y , and is also invariant under the shift $(x, y) \mapsto (x + \pi, y + \pi)$; this also holds for the perturbation \mathbf{f} . So, we can take the rectangle $[-\frac{\pi}{2}, \frac{\pi}{2}] \times [-\frac{\pi}{2}, \frac{3\pi}{2}]$ with the sides identified by the shifts

$$(x, y) \mapsto (x + \pi, y + \pi), \quad (x, y) \mapsto (x, y + 2\pi) \quad (3.3)$$

as a fundamental domain for both the unperturbed Hamiltonian system $\dot{\mathbf{x}} = \mathbf{v}(\mathbf{x})$ and the perturbed system (3.2). We will refer to the torus resulting from taking the factor over (3.3) as \mathbb{T}^2 . This reduces the original four-dimensional system (1.1) to the flow (3.2) on the torus \mathbb{T}^2 . The flow in \mathbb{R}^4 decomposes into the product of the periodic flow (3.2) on \mathbb{R}^2 and a contraction in transversal \mathbb{R}^2 -fibers.

3.2 Poincaré map

Choice of a transversal. Assuming $b > 0$, the vertical lines $\tilde{T}_k = \{(x, y) \in \mathbb{R}^2, x = \pi k - \frac{\pi}{2}\}$, $k \in \mathbb{Z}$ are transversal to the Hamiltonian flow by (2.1) since $\dot{x} = b$ there. This transversality survives for all ε sufficiently small in the perturbed flow (3.2). We choose \tilde{T}_k as Poincaré sections for the flow on \mathbb{R}^2 ; on the torus they all correspond to the same circle that we denote T . Let us use

$$z = \frac{y - x}{2\pi}$$

as a coordinate on each \tilde{T}_k . As z is invariant under the shift $(x, y) \mapsto (x + \pi, y + \pi)$ identifying \tilde{T}_k with \tilde{T}_{k+1} , it is a well-defined coordinate on T , and it turns T into the *standard* circle $\mathbb{R}/\mathbb{Z} = S^1$. Let $P : S^1 \mapsto S^1$ denote the first return map to T . P is an increasing degree one circle map since different trajectories of (3.2) do not

⁷The required smallness of ε depends on r .

intersect. However, P is undefined at certain points (we will later see that there are two such points). Now, assume $b > 0$. Then P has a natural lift $\tilde{P} : \mathbb{R} \mapsto \mathbb{R}$ which is the Poincaré map from \tilde{T}_k to \tilde{T}_{k+1} using z as a coordinate on both transversals. It does not depend on k as both z and the flow are invariant by the shift $(x, y) \mapsto (x + \pi, y + \pi)$.

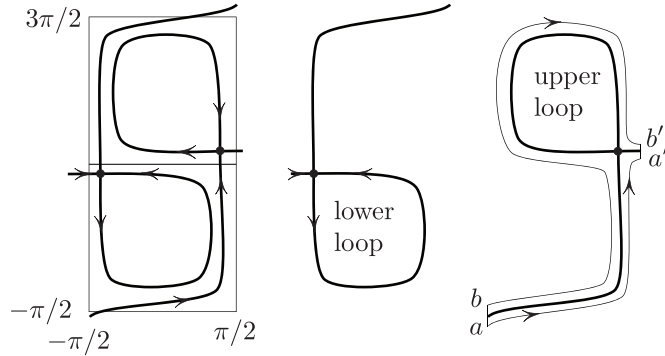


Figure 8: The first return map P_0 of the Hamiltonian system is continuous: $\lim_{|ab| \rightarrow 0} |a'b'| = 0$.

Hamiltonian flow: the first return map is a pure rotation. Here we briefly describe the unperturbed flow (1.2) on the torus when $a, b \in (0, 0.1)$; proofs can be found in Appendix B. Let P_0 be the first return map for the Hamiltonian flow, and let \tilde{P}_0 be a lift of P_0 to the real line. This flow has two saddles, each having one homoclinic loop (Figure 8). The first return map P_0 is defined everywhere except for two points where stable manifolds of the saddles intersect the transversal T . A formula for P_0 arises from the fact that the Hamiltonian H is preserved by the flow. Let us choose H as the coordinate on \tilde{T}_0 ; since $\cos x \cos y = 0$ on \tilde{T} , $H(p_0)$ is a linear function of z_0 . Let $p_1 \in \tilde{T}_1$ be the translate of $p_0 \in \tilde{T}_0$ under $(x, y) \mapsto (x + \pi, y + \pi)$. Then

$$\underbrace{H(p_0)}_{Z_0} = \underbrace{H(p_1) + \pi a - \pi b}_{Z_1}.$$

Since $H(p_0) = Z_0$ is already chosen as the coordinate of p_0 , for consistency we must choose the right-hand side Z_1 to be the coordinate of $p_1 \in \tilde{T}_1$. Now if $\hat{p}_0 \in \tilde{T}_0$ and $\hat{p}_1 \in \tilde{T}_1$ lie on the same trajectory then $H(\hat{p}_0) = H(\hat{p}_1)$ and hence their coordinates relate as

$$\hat{Z}_1 = \hat{Z}_0 + \pi a - \pi b,$$

showing that the circle map is a rotation. Scaling by $2b\pi$ to return to z -coordinate gives an exact formula for this rotation:

$$\tilde{P}_0 : \mathbb{R} \mapsto \mathbb{R}, \quad z \mapsto z + \frac{a - b}{2b}. \quad (3.4)$$

To put this observation in a general context, note that Arnold showed [26] that under mild genericity conditions a general area-preserving flow on the 2-torus (i.e., a flow given by a multivalued Hamiltonian such as the one we consider) admits a transversal, and the first return map is undefined only at finitely many point and is a pure rotation on its domain. In our example a transversal exists a priori for all a, b (except $a = b = 0$), so no extra conditions are needed.

Perturbed flow: the first return map has two jumps. As ε increases from zero, each of the two homoclinic loops in Figure 8 opens up as illustrated in Figure 9, giving rise to a jump discontinuity, Figure 10a. The jumps are the intervals on the transversal where trajectories escaping from former homoclinic loops merge into the flow (I_1 and I_2 in the figure on the right). These intervals are bounded by two branches of the unstable manifold of a saddle. The points of discontinuity of the return map (points b_1 and b_2 in Figure 9, right) are the intersections of the stable manifolds of the saddles with the transversal.

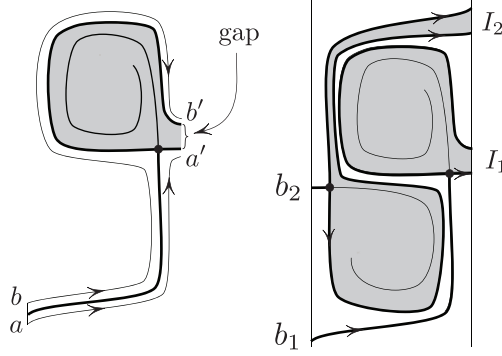


Figure 9: When $\varepsilon > 0$, the first return map P has two jump discontinuities. For starting points a, b separated by the stable manifold we have $\lim_{|ab| \rightarrow 0} |a'b'| > 0$.

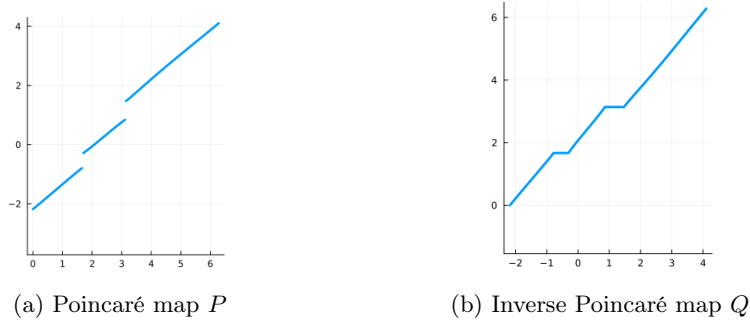


Figure 10: Circle maps describing the particle dynamics

3.3 Construction of the family of circle maps.

In order to work with continuous maps, it will be convenient to consider the inverse Poincaré map, Figure 10b. The proposition below claims that fixing b and ε and changing a makes this inverse Poincaré map a monotone family of circle maps with two flat spots. We actually need to take $s = -a$ as the parameter to make the resulting family increasing rather than decreasing.

Assuming that the phase portrait in Figure 9 is valid, set the circle map Q to be the inverse-time first return map of the flow (3.2) on $S^1 \setminus (I_1 \cup I_2)$, extending the map to the full circle by setting $Q(I_1) = b_1$ and $Q(I_2) = b_2$. The resulting map Q is a continuous non-decreasing circle map. Let $s = -a$ be the parameter and fix b and ε . This gives a family of circle maps Q_s .

Proposition 3.2. *There exists $\gamma > 0$ such that for any positive $\delta < \gamma$ there exists $\varepsilon_0 > 0$ such that*

1. *For any a and $b \in [\delta, \gamma]$ with $a \leq 1.5b$ and any $\varepsilon \in (0, \varepsilon_0)$ the phase portrait of the flow (3.2) on the 2-torus $[-\frac{\pi}{2}, \frac{\pi}{2}] \times [-\frac{\pi}{2}, \frac{3\pi}{2}]$ factorized by (3.3) is as in Figure 9, more precisely:
 - (a) *This flow has two saddles, two sources, and no other fixed points.*
 - (b) *The forward trajectory of any point that is not on a stable manifold of a saddle and is not one of the sources intersects T .*
 - (c) *The inverse-time first return map Q is defined and continuous on the whole circle T except for two closed intervals I_1, I_2 . Each of these intervals is bounded by an intersection of the two unstable manifolds of a saddle with T . One-sided limits of this map at the endpoints of such interval I_j exist and coincide with the point the points b_j ($j = 1, 2$) where the stable manifold of the same saddle intersects T .**
2. *Fix $b \in [\delta, \gamma]$ and $\varepsilon \in (0, \varepsilon_0)$. Treat $s = -a$ as a parameter. Then the family $Q_s(z)$, $s \in [-\gamma, -\delta]$ is a monotone family of circle maps with two flat spots (in the sense of Definition 1.2).*

Moreover, the expansion constant λ in the definition of a monotone family can be taken to be greater than $1 + c\varepsilon$, where $c > 0$ depends only on δ .

This proposition is proved in Section 5.

Remark 3.3. *Since the value of the Hamiltonian of the unperturbed system changes by $O(\varepsilon)$ while the trajectory starting on the transversal returns there (this is proved in the appendices, Remark E.14), the Poincaré map P of the perturbed system is $O(\varepsilon)$ -close to the rigid rotation (3.4) in C^0 . The argument with the change of the Hamiltonian works for the time-reversed flow as well, so the map Q is also $O(\varepsilon)$ -close to a rotation in C^0 , namely, to the inverse of the map (3.4).*

Rotation number and the drift slope. The next statement relates the rotation number of the first return map P to the asymptotic slope of the trajectory: one is a linear function of the other.

Remark 3.4. *For an initial point $\mathbf{x}_0 = (x_0, y_0) \in \tilde{T}$, let $z_0 = \frac{y_0 - x_0}{2\pi} \in \mathbb{R}$; suppose that z_0 has an infinite future P -orbit. Then*

1. *The rotation number*

$$\rho = \lim_{n \rightarrow \infty} \frac{\tilde{P}^n(z_0) - z_0}{n}$$

exists.

2. *The forward trajectory $\mathbf{x}(t)$ of (3.2) starting at \mathbf{x}_0 is unbounded and at a finite distance from a ray with the slope $2\rho + 1$.*

Apart from the particular formula connecting drift slope with rotation number, this is a well-known general fact on torus flows. A proof is given in Appendix D.

3.4 Proof of Theorem 1.1.

Now we are ready to prove Theorem 1.1 modulo Theorem 1.3, propositions 3.1 and 3.2, and Remark 3.4.

Proof of Theorem 1.1. Let us first pick the constants in Theorem 1.1. We take γ as in Proposition 3.2 and take $\varepsilon_0(\delta)$ to be the smaller of the two values: $\varepsilon_0(\delta)$ from Proposition 3.2 and ε_0 from Proposition 3.1 with $M = \gamma$. For this choice of constants, we have conclusions of both propositions when $a, b \in [\delta, \gamma]$ and $\varepsilon \in (0, \varepsilon_0)$.

By Proposition 3.1, the evolution of the particle's position $\mathbf{x}(t)$ governed by the 4-dimensional flow (1.1), (1.2) is captured by the torus flow (3.2), since this invariant torus is globally attracting. The entire phase space is foliated by fibers with base points on the invariant torus; the flow is the product of contraction in the fiber and the flow on the torus \mathcal{M}_ε .

The phase portrait of the torus flow (3.2) is described by the first part of Proposition 3.2. There are two sources, two saddles, and no other fixed points. Take a point $p \in \mathcal{M}_\varepsilon \simeq \mathbb{T}^2$ that is not one of the sources and is not on the stable manifold (winding around the torus) of one of the saddles. The forward orbit of p then intersects the transversal T , as claimed in Proposition 3.2; repeating this argument shows that it intersects T infinitely many times. According to Remark 3.4, the lift of this forward trajectory to \mathbb{R}^2 is unbounded and at a finite distance of a ray with the slope $m = 2\rho + 1$, where ρ is the rotation number of this orbit under the first return map \tilde{P} . Recall that the circle map Q defined in Section 3.3 above denotes the inverse-time first return map continued to be constant on the two intervals where it is undefined, and $\tilde{Q} : \mathbb{R} \mapsto \mathbb{R}$ is its lift. Proposition 3.2 claims that it is a continuous non-decreasing degree one circle map (this is included in Definition 1.2), so it has a rotation number $\rho(\tilde{Q})$. Clearly, this implies that for any forward-unbounded trajectory $\rho(\tilde{P}) = -\rho(\tilde{Q})$, and the particle drift slope is $m = 1 - 2\rho(\tilde{Q})$ for all initial data on the stable fiber of the points on \mathcal{M}_ε projecting to the point p on the torus. So, the particle drift slope exists and equals $1 - 2\rho(\tilde{Q})$ for all initial data in \mathbb{R}^4 except for countably many two-dimensional manifolds (projecting to the sources on the torus) and countably many three-dimensional manifolds projecting to the

stable manifolds of the saddles. These three-dimensional manifolds coincide with the stable manifolds of the saddles for the ODE in \mathbb{R}^4 .

We have checked that the particle drift slope m is well defined for most initial data and does not depend on the initial point. Moreover, $m = 1 - 2\rho(\tilde{Q})$. Fixing b and ε and parametrizing the map Q by $s = -a$ gives rise to a circle map family \tilde{Q}_s . By Proposition 3.2, \tilde{Q}_s is a monotone family (Definition 1.2), and its rotation number as a function of s satisfies the conclusions of Theorem 1.3. So, the same properties also hold for the particle drift slope $m(\alpha)$ parametrized by $\alpha = a/b$. Indeed, $m(\alpha) = 1 - 2\rho(\tilde{Q}_s|_{s=-\alpha b})$. This gives the properties of the function $m(\alpha)$ claimed in Theorem 1.1. \square

4 Circle maps with flat spots

In this section we prove Theorem 1.3. Consider a monotone (in sense of Definition 1.2) family f_s of circle maps with $m > 0$ flat spots. Fix a lift $\tilde{f}_s : \mathbb{R} \mapsto \mathbb{R}$. The following lemma summarizes some known results from [33] and from references therein.

Lemma 4.1.

1. Each f_s has a well-defined and unique rotation number $\rho(s) = \rho(\tilde{f}_s)$.
2. $\rho(s)$ depends continuously on the parameter s .
3. $\rho(s)$ is non-decreasing in s and strictly increasing when ρ is irrational.
4. When $\rho(s)$ is rational, it is constant on a non-degenerate closed interval of s -values.

For the sake of completeness and to deal with the fact that Definition 1.2 is a bit different from the class of circle maps families considered in [33], we provide a proof in Appendix D.

Lemma 4.1 implies the first three conclusions of Theorem 1.3. Let us now prove Conclusion 4 claiming that $\dim_H(C) = 0$. Conclusion 5 (steepness) will be a side result of this. The key idea is to use the expansivity in a way similar to Veerman's proof for the case of one flat spot [33]. This is done below in the proof of Lemma 4.2. But then instead of estimating the lengths of intervals in the complement to C , as done by Boyd [31] and later Veerman, we write $C = \bigcap_N C_N$ and estimate the lengths of the intervals in C_N . This gives a shorter proof, as there is no need to prove that C has zero measure prior to proving that it has zero Hausdorff dimension.

Let \tilde{I}_j be lifts of the flat spots I_j , and let $\tilde{b}_j(s) = \tilde{f}_s(I_j(s))$. For a positive integer N let C_N be the set of all parameters s such that the rotation number is irrational or rational with the denominator greater than mN :

$$C_N = \left\{ s \in [s_{min}, s_{max}] : \rho(s) \notin \mathbb{Q} \text{ or } \rho(s) = \frac{p}{q} \in \mathbb{Q} \text{ with } \gcd(p, q) = 1, q > mN \right\}.$$

Clearly, $C = \bigcap_{N=1}^{\infty} C_N$.

The following lemma and its corollary are used to estimate the Hausdorff dimension and the steepness of ρ .

Set⁸

$$\psi_N(s) = \sum_{j=1}^m \tilde{f}_s^{N-1}(\tilde{b}_j(s)). \quad (4.1)$$

Lemma 4.2. *Pick any $s_0 \in C_N$. Then the 'slope' of $\psi(s)$ near s_0 is $\gtrsim \lambda^N$. More formally, there exists $\delta > 0$ such that for any $\tau_1, \tau_2 \in [s_0 - \delta, s_0 + \delta]$ with $\tau_2 \geq s_0 \geq \tau_1$ we have*

$$\psi(\tau_2) - \psi(\tau_1) \geq \nu \lambda^{N-1} (\tau_2 - \tau_1), \quad (4.2)$$

where the constants λ and ν are from Definition 1.2: $\lambda > 1$ is the expansion constant, and $\nu > 0$ is a lower bound on $\frac{d\tilde{b}_j}{ds}$.

⁸This generalizes the function $\frac{1}{N} \tilde{f}_s^{N-1}(\tilde{b}_1(s))$ Veerman considered for one flat spot.

Proof. Set $\mathcal{I}(s) = \cup_{j=1}^m I_j(s)$. First, let us show that for some j we have

$$f_{s_0}^n(b_j(s_0)) \notin \mathcal{I}(s_0), \quad n = 0, 1, \dots, N-1. \quad (4.3)$$

Suppose the opposite holds, so that for any j there exist $k_j \leq m$ and $n_j \leq N-1$ such that $f_{s_0}^{n_j}(b_j(s_0)) \in I_{k_j}(s_0)$. Let us write $j \mapsto k_j$ if this is the case. As there are only m flat spots, by the pigeonhole principle we can find a cycle

$$j_1 \mapsto j_2 \mapsto \dots \mapsto j_q \mapsto j_1, \quad q \leq m.$$

As $j_s \mapsto j_{s+1}$ implies $f_{s_0}^{n_{j_s}+1}(b_{j_s}) = b_{j_{s+1}}$, this shows that f_{s_0} has a periodic orbit with the period

$$(n_{j_1} + 1) + \dots + (n_{j_q} + 1) \leq qN \leq mN.$$

Then, $\rho(s_0)$ is rational with the denominator $\leq mN$, which contradicts $s_0 \in C_N$. This contradiction shows that (4.3) holds for some j .

Now, fix j such that we have (4.3). By the continuity of $I_j(s)$, for some $\delta > 0$ for any $s \in [s_0 - \delta, s_0 + \delta]$ we also have (4.3) with $b_j(s)$ instead of $b_j(s_0)$ (while we still iterate f_{s_0}):

$$f_{s_0}^n(b_j(s)) \notin \mathcal{I}(s_0), \quad n = 0, 1, \dots, N-1. \quad (4.4)$$

Let us now fix $\tau_1, \tau_2 \in [s_0 - \delta, s_0 + \delta]$ with $\tau_1 \leq s_0 \leq \tau_2$ and prove (4.2). As all the summands in (4.1) are monotone with respect to s , it is enough to prove that for j picked above

$$\tilde{f}_{\tau_2}^{N-1}(\tilde{b}_j(\tau_2)) - \tilde{f}_{\tau_1}^{N-1}(\tilde{b}_j(\tau_1)) \geq \nu \lambda^{N-1}(\tau_2 - \tau_1). \quad (4.5)$$

This is done using expansivity as in Veerman's lemmas 5.1 and 5.2. We have $\tilde{b}_j(\tau_2) - \tilde{b}_j(\tau_1) \geq \nu(\tau_2 - \tau_1)$ due to property 5 of monotone families. By monotonicity, we have

$$\tilde{f}_{\tau_2}^{N-1}(\tilde{b}_j(\tau_2)) - \tilde{f}_{\tau_1}^{N-1}(\tilde{b}_j(\tau_1)) \geq \tilde{f}_{s_0}^{N-1}(\tilde{b}_j(\tau_2)) - \tilde{f}_{s_0}^{N-1}(\tilde{b}_j(\tau_1)).$$

For any $n \leq N-1$ the arc $[f_{s_0}^n(\tilde{b}_j(\tau_1)), f_{s_0}^n(\tilde{b}_j(\tau_2))]$ does not intersect $\mathcal{I}(s_0)$. Indeed, by the intermediate value theorem any x in this arc can be written as $x = f_{s_0}^n(\tilde{b}_j(s)) \notin \mathcal{I}(s_0)$, with $s \in [\tau_1, \tau_2]$. Thus, due to the expansivity outside of \mathcal{I} we get

$$\tilde{f}_{s_0}^{N-1}(\tilde{b}_j(\tau_2)) - \tilde{f}_{s_0}^{N-1}(\tilde{b}_j(\tau_1)) \geq \lambda^{N-1}(\tilde{b}_j(\tau_2) - \tilde{b}_j(\tau_1)) \geq \nu \lambda^{N-1}(\tau_2 - \tau_1).$$

□

Corollary 4.3. *Any interval $[s_1, s_2] \subset C_N$ satisfies*

$$s_2 - s_1 \leq KN \lambda^{-N} \quad (4.6)$$

for some constant K independent of N .

Proof. We will construct a sequence $s_1 = y_0 < y_1 < \dots < y_L = s_2$ so that we can estimate $\psi(y_{i+1}) - \psi(y_i)$ using Lemma 4.2. To this end, cover each $s \in [s_1, s_2]$ by its δ -neighborhood provided by Lemma 4.2. Select a finite subcover $\{\tilde{U}_i\}$ and remove all intervals contained inside another interval. Let $\{U_i\}$, $i = 1, \dots, L$ denote the resulting subcover reordered so that the centers form an increasing sequence. Then, U_i intersects U_{i+1} for any i (otherwise, the interval U_j covering the empty space between them will cover U_i if $j < i$ or U_{i+1} if $j > i+1$). Set $y_0 = s_1$. When $i = 1, \dots, L-1$, set y_i to be any point in $U_i \cap U_{i+1}$ lying between the centers of U_i and U_{i+1} . Finally, set $y_L = s_2$. By construction, $[y_i, y_{i+1}]$ is covered by U_{i+1} for any $i = 0, \dots, L-1$ and contains the center of U_{i+1} . Thus, Lemma 4.2 implies $\psi(y_{i+1}) - \psi(y_i) \geq \nu \lambda^{N-1}(y_{i+1} - y_i)$. Adding these inequalities together yields

$$\psi(s_2) - \psi(s_1) \geq \nu \lambda^{N-1}(s_2 - s_1).$$

As f has degree one, there is $M > 0$ such that for any $N \geq 1$ and any j we have $|\tilde{f}_s^N(\tilde{b}_j)| < MN$ for all s . This implies $|\psi(s)| \leq MmN$ and $\psi(s_2) - \psi(s_1) \leq 2MmN$. Combining with the previous inequality yields the estimate on $s_2 - s_1$. □

Now, we are ready to prove steepness. For right endpoints, steepness follows from the corollary below. For left endpoints, it can be proved in the same way.

Corollary 4.4. *Let s_0 be a right endpoint of some rational interval $\{s : \rho(s) = \frac{p}{q}\}$. Then, for all small enough $s > 0$ we have*

$$\rho(s_0 + s) - \rho(s_0) > \frac{D}{q|\ln s|}, \text{ where } D = \frac{\ln \lambda}{4m}. \quad (4.7)$$

Proof. By Corollary 4.3 for large enough N the length of each interval contained in C_N is less than $\lambda^{-N/2}$. Assuming s is small enough, take $N = 2\lceil \frac{-\ln s}{\ln \lambda} \rceil + 2$. Then $N \geq -2 \log_\lambda s$, and $\lambda^{-N/2} \leq s$. Then $(s_0, s_0 + s)$ cannot be a subset of C_N , and so there is $s' \in (s_0, s_0 + s)$ with $\rho(s')$ being rational with the denominator $Q \leq mN$. Hence, $\rho(s') - \rho(s_0) \geq \frac{1}{qQ} \geq \frac{1}{qmN}$.

Provided that s is small enough, we have $N \leq 4\lceil \frac{|\ln s|}{\ln \lambda} \rceil$ and thus $\rho(s') - \rho(s_0) \geq \frac{\ln \lambda}{4qm|\ln s|}$, as claimed. \square

Before we estimate the Hausdorff dimension of C , let us recall the definition. For $d > 0$ and a finite or countable union \mathcal{U} of closed intervals U_i denote $m_d = \sum_i |U_i|^d$ and $\text{diam } \mathcal{U} = \sup_i |U_i|$. The d -dimensional *Hausdorff measure* of a set X is defined as

$$\mathcal{H}^d(X) = \sup_{\delta > 0} \inf \{m_d(\mathcal{U}) : \text{diam } \mathcal{U} < \delta \text{ and } \mathcal{U} \text{ covers } X\},$$

and the *Hausdorff dimension* of X is

$$\dim_H(X) = \inf \{d \geq 0 : \mathcal{H}^d(X) = 0\}.$$

Note that C_N is a finite union of intervals, and let \mathcal{U}_N be the union of the closures of these intervals.

Lemma 4.5.

$$m_d(\mathcal{U}_N) = O(N^{2+d})(\lambda^d)^{-N}, \quad \text{diam } \mathcal{U}_N = O(N\lambda^{-N}),$$

where the constants in the O -estimates do not depend on N .

Proof. The estimate on $\text{diam } \mathcal{U}_N$ follows from Corollary 4.3. The number of intervals in \mathcal{U}_N is $O(N^2)$, as there are $O(N^2)$ rational numbers with the denominator $\leq mN$ in any fixed interval. Together with the estimate on $\text{diam } \mathcal{U}_N$ this gives the estimate on $m_d(\mathcal{U}_N)$. \square

This lemma implies that for any $d > 0$, when $N \rightarrow \infty$, we have $m_d(C_N) \rightarrow 0$ and $\text{diam } C_N \rightarrow 0$. Thus, $\mathcal{H}^d(C) = 0$, and $\dim_H(C) = 0$. This completes the proof of Theorem 1.3.

5 Proof of monotonicity of the circle map family

The first part of Proposition 3.2 is proved in Appendix E.2. Here we prove the second part of the proposition using the first part as well as several technical lemmas proved below in appendices. We need to verify that for fixed b and ε the family $Q_s(z)$ defined in Section 3.3 satisfies properties 1-5 in Definition 1.2, treating $s = -a$ as the parameter.

1a. Continuity: $Q_s(z)$ is continuous with respect to both z and s . The continuity in z is stated in conclusion (c) of the first part of Proposition 3.2. The continuity with respect to s when z is outside the flat spots follows from continuous dependence of solutions of the ODE (3.2) with reversed time with respect to the parameter s . When z is inside a flat spot, continuity in s can be deduced from continuity in s outside the flat spots and monotonicity and continuity in z . Indeed, take any value s_0 of the parameter and any point $z \in \mathbb{R}$ lying in a flat spot (more precisely, in its lift to \mathbb{R}). Let $J \subset \mathbb{R}$ be a connected component of the lift of a flat spot that covers z . Set $z' = \tilde{Q}_{s_0}(z)$. Take two points $a, b \in \mathbb{R}$ outside flat spots so that for $s = s_0$ the interval $[a, b]$ covers J but a and b are so close the two endpoints of J

that $|\tilde{Q}_{s_0}(a) - z'| < \varepsilon/2$ and $|\tilde{Q}_{s_0}(b) - z'| < \varepsilon/2$. By the continuity in s outside flat spots, for any s_1 close enough to s_0 we have $|\tilde{Q}_{s_1}(a) - z'| < \varepsilon$ and $|\tilde{Q}_{s_1}(b) - z'| < \varepsilon$. As $\tilde{Q}_{s_1}(z)$ is between $\tilde{Q}_{s_1}(a)$ and $\tilde{Q}_{s_1}(b)$, this implies the continuity of $Q_s(z)$ at s_0 .

1b. Monotonicity $\tilde{Q}_s(z)$ in z follows from the fact that trajectories of (3.2) do not intersect each other.

Monotonicity with respect to the parameter s is much less obvious, and it is helpful to establish the other properties first so that they can be used to prove monotonicity in s . This is done below under the name “property 1c”.

2. Degree one: Q_s has degree 1 for all s . As the vector field (3.2) is periodic and solutions of the corresponding ODE are unique, two solutions starting at the points (x_0, y_0) and $(x_0, y_0 + 2\pi)$ are related by the vertical shift by 2π . Hence, for any two points on the transversal (which is vertical) their images under the inverse-time Poincaré map \tilde{Q}_s also differ by the same shift.

3. Flat spots: there are two flat spots for each s . More precisely, there are two disjoint closed arcs $I_1(s)$ and $I_2(s)$ such that Q_s is constant on each arc. The endpoints of these arcs depend on s continuously. Existence of two flat spots follows from the construction of Q_s described in Section 3.2. Indeed, by the first part of Proposition 3.2 there are two intervals I_1 and I_2 bounded by saddle separatrices (Figure 8) such that outside these intervals time-reversed Poincaré map is defined, and we set Q_s to be constant on these intervals. The continuity of the endpoints of $I_1(s)$ and $I_2(s)$ with respect to s follows from the continuous dependence of the separatrices on s and their transversality to the Poincaré section.

4. Expansivity: There exists $\lambda > 1$ such that for each s the map Q_s is λ -expanding outside $I_1 \cup I_2$. Namely, if $z \notin I_1 \cup I_2$ and $z \in \mathbb{R}$ is any lift of z , $\tilde{f}_s(z)$ is differentiable in z and $\frac{d}{dz}(\tilde{f}_s(z)) > \lambda$. Moreover, we can take $\lambda > 1 + c\varepsilon$ with $c > 0$ depending only on the constant δ bounding from below a and b (recall the assumption $a, b > \delta > 0$ in Proposition 3.2).

This follows from the following lemma proved below in Appendix E.4.

Lemma 5.1. *There exists $\gamma > 0$ such that for any positive $\delta < \gamma$ there exist $\varepsilon_0 > 0$ such that for any $a, b \in (\delta, \gamma)$ and for any positive $\varepsilon < \varepsilon_0$ the map P is contracting except for the two points where it has a jump discontinuity (Figure 9):*

$$\frac{d}{dz}P(z) < 1 - \varepsilon.$$

As Q is inverse to P outside the flat spots, this implies expansivity for Q :

$$\frac{d}{dz}Q = \left(\frac{d}{dz}P\right)^{-1} > (1 - \varepsilon)^{-1} > 1 + \varepsilon.$$

5. Flat spots heights increase with the parameter: $\frac{d}{ds}\tilde{b}_j(s) > 0.15$ for all $s, j = 1, 2$. As $s = -a$, this follows from the following lemma proved below in Appendix E.3.

Lemma 5.2. *For any positive $\delta < 0.05$ there exists $\varepsilon_0 > 0$ such that for any $a, b \in (\delta, 0.1 - \delta)$ and any positive $\varepsilon < \varepsilon_0$,*

$$\frac{\partial}{\partial a}\tilde{b}_j(a, b, \varepsilon) < -0.15.$$

1c. Monotonicity in the parameter: $\tilde{Q}_s(z)$ is non-decreasing with respect to s . We need the following lemma, proved in Appendix E.5. Recall that $\tilde{P} : \mathbb{R} \mapsto \mathbb{R}$ denotes the forward-time Poincaré map (Section 3.2); $\tilde{P} = \tilde{P}_{a,b,\varepsilon}$ depends on the parameters a, b , and ε .

Lemma 5.3. *The exists $\gamma > 0$ such that for any positive $\delta < \gamma$ there exists $\varepsilon_0 > 0$ such that for any $a, b \in (\delta, \gamma)$ and for any positive $\varepsilon < \varepsilon_0$,*

$$\frac{\partial}{\partial a}\tilde{P}(z) > 0,$$

provided that $z \in \mathbb{R}$ is such that $\tilde{P}(z) = \tilde{P}_{a,b,\varepsilon}(z)$ is defined.

Now we can prove monotonicity of $\tilde{Q}(z)$ with respect to $s = -a$. If z is outside the flat spots, it follows from Lemma 5.3, as \tilde{Q} is (locally) the inverse of \tilde{P} . By continuity, this also implies that \tilde{Q} is non-decreasing in s if z is on the boundary of a flat spot. Finally, monotonicity for z strictly inside a flat spot follows from the monotonicity of flat spots' heights discussed above. \square

Appendix A Incorporating external force in the fluid velocity field

In this appendix we show how adding an external force acting on a particle carried by fluid flow results in the model (1.1), (1.2) we consider. This model was proposed by Maxey and Corrsin [7], and the discussion below follows their paper.

Let $\mathbf{u}(\mathbf{x})$ be the fluid velocity at the point \mathbf{x} , and let the constant vector \mathbf{g} be the free fall acceleration. A simplified form of Maxey-Riley equation is Newton's second law for the position $\mathbf{x}(t)$ of a spherical aerosol particle carried by the fluid and pulled by gravity:

$$m\ddot{\mathbf{x}} = -k(\dot{\mathbf{x}} - \mathbf{u}(\mathbf{x})) + m\mathbf{g},$$

where m is the particle mass and k is the drag coefficient; for spherical particles $k = 6\pi a\mu$ where a is the radius and μ is the fluid viscosity. Setting $\mathbf{w} = m\mathbf{g}/k$ (this vector can be interpreted as the terminal velocity of the particle in a still fluid) and letting $\mathbf{v} = \mathbf{u} + \mathbf{w}$ gives

$$m\ddot{\mathbf{x}} = -k(\dot{\mathbf{x}} - \mathbf{v}(\mathbf{x})).$$

Finally, dividing by m and setting $\varepsilon = m/k = m/(6\pi a\mu)$ yields the model (1.1), (1.2):

$$\ddot{\mathbf{x}} = -\frac{1}{\varepsilon}(\dot{\mathbf{x}} - \mathbf{v}(\mathbf{x})),$$

where

$$\mathbf{v} = \mathbf{u} + \mathbf{w}, \quad \varepsilon = m/(6\pi a\mu), \quad \mathbf{w} = m\mathbf{g}/(6\pi a\mu).$$

This shows that adding external force is equivalent to modifying the "carrying" vector field.

Appendix B Properties of the Hamiltonian flow

In this appendix, we establish several properties of the Hamiltonian flow \mathbf{v} , (1.2) and (2.1). For brevity, we will refer to the two branches of the invariant manifold of a saddle as *separatrices* throughout this appendix. Accordingly, in our notation, each saddle has two stable separatrices and two unstable ones.

Consider the grid $\Gamma = \{(k_1\pi + \frac{\pi}{2}, k_2\pi + \frac{\pi}{2}), k_1, k_2 \in \mathbb{Z}\}$ formed by the saddles of this flow when $a = b = 0$ so that $H = \cos x \cos y$. When a and b are small, the actual saddles are close to the nodes of Γ , and we index these saddles by the nearest nodes of Γ . We shall say that a saddle of \mathbf{v} is *odd* if $k_1 + k_2$ for the nearest node of Γ is odd, and *even* otherwise.

Lemma B.1. *Suppose $0 \leq a, b \leq 0.1$. Then, the Hamiltonian (1.2) at a saddle of \mathbf{v} is*

$$H = by_\Gamma - ax_\Gamma \pm K \tag{B.1}$$

with the plus sign if the saddle is odd and the minus sign if it is even. Here x_Γ, y_Γ are the coordinates of the nearest node of Γ , and

$$K = \frac{1}{2}(f(b-a) - f(b+a)) \quad \text{with } f(x) = \sqrt{1-x^2} + x \arcsin x. \tag{B.2}$$

Proof. It is convenient to rewrite

$$H = \frac{1}{2}(\cos(x+y) + \cos(x-y)) + by - ax$$

and use $X = x+y, Y = x-y$ as new variables⁹. Then, $x = \frac{X+Y}{2}, y = \frac{X-Y}{2}$, and

$$H = \frac{1}{2}(\cos X + \cos Y + (b-a)X - (a+b)Y). \tag{B.3}$$

A straightforward computation yields the coordinates of the odd saddles:

$$X = \arcsin(b-a) + 2\pi k, \quad Y = \pi + \arcsin(a+b) + 2\pi l$$

⁹This is not a canonical transformation, but we will not write the Hamilton equations in the new coordinates; we just want to find the saddle points of the function H .

and of the even saddles:

$$X = \pi - \arcsin(b - a) + 2\pi k, \quad Y = -\arcsin(a + b) + 2\pi l.$$

Substitution into (B.3) yields (B.1). \square

“Chess” game rule – the proof. Here we prove that the forward-unbounded trajectories of \mathbf{v} wind their way according the combinatorial “Chess game” rule stated in Section 2. It is clear that when a and b are small, unbounded trajectories are close to the edges of Γ and turn near its vertices. Trajectories turning left and right are separated by the stable manifold of the nearby saddle of \mathbf{v} ; solutions precisely on the separatrix are bounded and thus are not considered. Consider an unbounded trajectory making a turn near a saddle. Let H_0 be the value of H on this trajectory, and let H_s be the value of H on the stable manifold which this trajectory follows before turning left or right as after approaching the saddle with the same value H_s of the Hamiltonian. And the turn direction is determined by the sign of $H_s - H_0$. The values of H_s are computed above in Lemma B.1, and the answer was different for odd and even saddles, this is the reason for the chess coloring used in the statement of the “Chess” rule. For an odd saddle near a node (x_Γ, y_Γ) , we have $H_s = by_\Gamma - ax_\Gamma + K$, so that a left turn happens if $by_\Gamma - ax_\Gamma + K < H_0$, while a right turn happens if $by_\Gamma - ax_\Gamma + K > H_0$. The equation of the line corresponding to odd vertices is thus $by - ax = c_o$ with $c_o = H_0 - K$; the turn is determined by the position of the grid node relative to this line. For even vertices, the same considerations work, but give another line: $by - ax = c_e$ with $c_e = H_0 + K$. \square

Lemma B.2. *For any $a, b \in (0, 0.1]$ the Hamiltonian flow \mathbf{v} has one saddle and one center in each cell $[-\frac{\pi}{2} + \pi k, \frac{\pi}{2} + \pi k] \times [-\frac{\pi}{2} + \pi l, \frac{\pi}{2} + \pi l]$ with $k, l \in \mathbb{Z}$. Two separatrices of the saddle form a homoclinic loop fully contained inside the cell, while two other separatrices do not form a loop (we shall call them free separatrices).*

If, additionally, $a \leq 1.5b$, then the free stable separatrix of the saddle intersects the transversal $x = -\frac{\pi}{2} + \pi k$ and the free unstable separatrix intersects the transversal $x = \frac{\pi}{2} + \pi k$. Moreover, the Poincaré map P_0 on the torus (Section 3.2) is defined at all points on the transversal other than the two points where free stable separatrices of the two saddles intersect the transversal.

Proof.

- *In each cell there are exactly two fixed points, one center and one saddle.*
This is a straightforward computation that can be done as in the proof of Lemma B.1.
- *One pair of separatrices of the saddle forms a homoclinic loop that lies inside the cell.* The cells we consider are the pieces \mathbb{R}^2 is divided into by a family of vertical lines and a family of horizontal lines. Restricted to the vertical lines $x = \frac{\pi}{2} + \pi k$, the horizontal component of \mathbf{v} on these lines is equal to b by (2.1). Vector field \mathbf{v} is transversal to the vertical lines $x = \frac{\pi}{2} + \pi k$ since $\dot{x} = b > 0$ there. Hence, these lines are transversal to \mathbf{v} , and all trajectories cross them all in one direction, from left to right. A similar statement holds for the horizontal lines $y = \frac{\pi}{2} + \pi k$ where $\dot{y} = a$. As each of these lines can only be crossed in one direction, periodic trajectories and homoclinic loops are only possible inside the cells.

The center is surrounded by periodic trajectories; the boundary of the domain formed by these trajectories must contain a critical point of H . This critical point is a fixed point of \mathbf{v} , so it must be the saddle. This means that the boundary of this domain is a homoclinic loop.

- *The other two pairs of separatrices does not form loops.*

If two other separatrices form another loop, one can find two periodic orbits near the two loops such that domains bounded by them are disjoint and do not contain the saddle. It is proved by considering two cases: if the interiors of the loops are disjoint and if the interior of one loop contains the other loop.

In each domain bounded by this two periodic orbits there is a fixed point by Poincaré-Hopf index theorem, which is a contradiction: there are only two fixed points, and the saddle is outside these domains by construction.

- Suppose that $a \leq 1.5b$. Then, *in any vertical strip $-\frac{\pi}{2} + \pi k \leq x \leq \frac{\pi}{2} + \pi k$, $k \in \mathbb{Z}$, all saddles have different values of the Hamiltonian H .* We can assume WLOG that $k = 0$, and the strip is $-\frac{\pi}{2} \leq x \leq \frac{\pi}{2}$. Denote this strip by Π . A straightforward computation shows that saddles in Π come in horizontal pairs, and different pairs are shifted vertically by $2\pi l$. These saddles are near the grid nodes $(-\frac{\pi}{2}, \frac{\pi}{2} + 2\pi l)$ and $(\frac{\pi}{2}, \frac{\pi}{2} + 2\pi l)$, where $l \in \mathbb{Z}$.

By Lemma B.1, the values of H at these saddles are $\frac{\pi}{2}(4bl + b \pm a) \mp K$ with " $-a$ " for the left saddle in each pair and " $+a$ " for the right one. As K is given by (B.2) and the function f there satisfies $f(0) = 1$ and $|f'| = |\arcsin x| < 0.3$ on $[-0.2, 0.2]$, we have $|K| < 0.3a$. Hence, the values of H at saddles with different l differ by at least $\frac{\pi}{2}(4b - 2a) - 2|K|$, which is positive as

$$\frac{\pi}{2}(4b - 2a) > 4b - 2a \geq 4b - 2 \cdot 1.5b \geq b \geq 0.6a > 2|K|.$$

The values of H at two saddles with the same l differ by at least $\frac{\pi}{2}(2a) - 2|K| > 0$.

- Suppose that $a \leq 1.5b$. Then, *free stable separatrix of the saddle intersects the transversal $x = -\frac{\pi}{2} + \pi k$ and free unstable separatrix intersects the transversal $x = \frac{\pi}{2} + \pi k$.*

Consider the vertical strip $-\frac{\pi}{2} + \pi k \leq x \leq \frac{\pi}{2} + \pi k$ containing the saddle and a rectangle R given by $-\frac{\pi}{2} + \pi k \leq x \leq \frac{\pi}{2} + \pi k$ and $|y| \leq M$, where the number M is so large that H restricted to the top side of R is greater than at the saddle, and H restricted to the bottom side of R is less than at the saddle. As \mathbf{v} goes right at the left and right sides of R , the free unstable separatrix can leave R only via its right side $x = \frac{\pi}{2} + \pi k$, and the free stable separatrix can leave R only via its left side $x = -\frac{\pi}{2} + \pi k$.

It remains to prove that free separatrices leave R , for definiteness let us prove that the free unstable separatrix cannot stay in R . Let p be any point on this separatrix inside R and let $\omega(p)$ be its ω -limit set. If the separatrix stays in R , we have $\omega(p) \subset R$. By Poincaré-Bendixson theorem, $\omega(p)$ can be either (1) a fixed point, (2) a periodic orbit, or (3) a union of fixed points and homoclinic or heteroclinic connections between them. As the sources are surrounded by periodic orbits, they cannot belong to $\omega(p)$. The only saddle that can belong to $\omega(p)$ is the "original" saddle whose separatrix we consider, as at other saddles the value of H is separated from the value of H on the orbit of p . However, because H is preserved at the orbit of p , it can only return near the original saddle along a separatrix. This would imply a homoclinic loop, which is not the case as the separatrix we consider is free. Finally, if $\omega(p)$ is a periodic orbit, the backward trajectory of p stays at these periodic orbit, while the backward trajectory of p actually approaches the saddle as p is on an unstable separatrix. This exhausts all possibilities. The resulting contradiction shows that the free unstable separatrix leaves R and so intersects the transversal $x = \frac{\pi}{2} + \pi k$.

- *The Poincaré map P_0 on the torus (Section 3.2) is defined at all points on the transversal other than the two points where stable separatrices of the two saddles intersect the transversal.* Consider the Poincaré map \tilde{P}_0 on \mathbb{R}^2 from the transversal $x = -\frac{\pi}{2}$ to the transversal $x = \frac{\pi}{2}$. We will prove that it is defined at all points other than the intersections of stable separatrices of the saddles in the strip Π given by $-\frac{\pi}{2} \leq x \leq \frac{\pi}{2}$ with the transversal $x = -\frac{\pi}{2}$. This will imply the statement about P_0 as \tilde{P}_0 projects to P_0 .

Consider a point p on the transversal $x = -\frac{\pi}{2}$ and suppose its orbit stays in the strip Π . Let us use Poincaré-Bendixson theorem as above to get a contradiction. The set $\omega(p)$ cannot be a periodic orbit as the orbit of p cannot return to the transversal $x = -\frac{\pi}{2}$. It cannot contain a source as those

are surrounded by periodic orbits. Finally, it cannot contain a saddle as $H(p)$ is different from the values of H at the saddle. Hence, the Poincaré map is defined at p . □

The following lemma will be used below to prove Lemma 5.2.

Lemma B.3. *Suppose $a, b \in (0, 0.1]$ with $a \leq 1.5b$. Let $y_1(a, b)$ and $y_2(a, b)$ be the y -coordinates of the intersections of the stable manifolds of the left and the right saddle, respectively, with the transversal $x = -\frac{\pi}{2}$. Then,*

$$\frac{\partial y_j}{\partial a} < -1, \quad j = 1, 2.$$

Proof. The values of the Hamiltonian H at $(-\pi/2, y_1)$ and $(-\pi/2, y_2)$ are the same as at the corresponding saddles. Denote these values by H_1 and H_2 , respectively. Since $x = -\pi/2$ on the transversal, we have $H_i = by_i + a\pi/2$, and

$$b \frac{\partial y_i}{\partial a} = \frac{\partial H_i}{\partial a} - \frac{\pi}{2}.$$

Using the formula for H_i from Lemma B.1, we get

$$\frac{\partial H_1}{\partial a} = \frac{\pi}{2} - \mu, \quad \frac{\partial H_2}{\partial a} = -\frac{\pi}{2} + \mu, \quad \text{where } \mu = \frac{1}{2} (\arcsin(b+a) + \arcsin(b-a)).$$

Hence,

$$b \frac{\partial y_1}{\partial a} = -\mu, \quad b \frac{\partial y_2}{\partial a} = -\pi + \mu.$$

As $|\mu| \leq \frac{\pi}{2}$, we we have $\frac{\partial y_2}{\partial a} \leq \frac{\partial y_1}{\partial a} = -\mu/b$. As $(\arcsin x)' \geq 1$, we have

$$\arcsin(b+a) + \arcsin(b-a) = \arcsin(b+a) - \arcsin(a-b) > 2b,$$

and $\mu > b$. Thus, $\frac{\partial y_2}{\partial a} \leq \frac{\partial y_1}{\partial a} < -1$. □

Appendix C Reduction to a torus flow - details

Sketch of a proof of Proposition 3.1. This sketch follows the book [41], and refers to theorems by Fenichel [40] as stated in this book. For clarity, we will first prove a weaker version where the required smallness of ε can depend on a and b and without checking that \mathbf{f} smoothly depends on a and b .

Rescaling the time by setting $t = \varepsilon\tau$ we turn (3.1) into

$$\mathbf{x}' = \varepsilon\mathbf{y}, \quad \mathbf{y}' = -(\mathbf{y} - \mathbf{v}(\mathbf{x})), \quad ' = \frac{d}{d\tau}. \quad (\text{C.1})$$

Now for $\varepsilon = 0$ the manifold \mathcal{M}_0 defined by $\mathbf{y} = \mathbf{v}(\mathbf{x})$ consists of critical points. It is normally hyperbolic center manifold with 2-dimensional contracting leaves. According to Fenichel's Theorem 1, for sufficiently small ε there exists an invariant manifold \mathcal{M}_ε that is smooth (including in ε), and C^r -close to \mathcal{M}_0 (where r depends on the smallness of ε). The local stable manifold $W^s(\mathcal{M}_\varepsilon)$ of \mathcal{M}_ε is 4-dimensional, so it contains a neighborhood of \mathcal{M}_ε . By Fenichel's Theorem 3, $W^s(\mathcal{M}_\varepsilon)$ is foliated by stable manifolds of different points of \mathcal{M}_ε , those are two-dimensional manifolds, and the exponential convergence holds. Now, note that for $\varepsilon = 0$ the manifold \mathcal{M}_0 is globally attracting, this means that the global stable manifold $W^s(\mathcal{M}_\varepsilon)$ is \mathbb{R}^4 , and all \mathbb{R}^4 is foliated by two-dimensional stable fibers. Finally, to get the dynamics on \mathcal{M}_ε , let us write \mathcal{M}_ε as a graph of a function

$$\mathbf{y} = \mathbf{v}(\mathbf{x}) + \varepsilon\mathbf{f}(\mathbf{x}, \varepsilon). \quad (\text{C.2})$$

The expression for f will come out of the condition that this graph is invariant under the flow C.1. Thus differentiating C.2 and using C.1 we obtain

$$-\underbrace{(\mathbf{y} - \mathbf{v}(\mathbf{x}))}_{\varepsilon\mathbf{f}} = \left(\frac{\partial \mathbf{v}}{\partial \mathbf{x}} + O(\varepsilon) \right) \mathbf{x}' = \varepsilon \frac{\partial \mathbf{v}}{\partial \mathbf{x}} \mathbf{v}(\mathbf{x}) + O(\varepsilon^2),$$

yielding

$$\mathbf{f} = -\frac{\partial \mathbf{v}}{\partial \mathbf{x}} \mathbf{v} + O(\varepsilon).$$

To show that smallness of ε can be taken uniformly over all a and b with $|a|, |b| < M$, one can consider a six-dimensional system treating a and b as slow variables with $\dot{a} = 0$ and $\dot{b} = 0$, then obtain a four-dimensional slow manifold for this system when ε is small enough, and then divide it into two-dimensional manifolds for different values of a, b . As the four-dimensional slow manifold is C^r , this also implies that \mathbf{f} smoothly depends on a and b . \square

Explicit formula for the perturbation. In the appendices below we study the perturbed system (3.2), which requires a more explicit formula for the perturbation \mathbf{f} . The general formula $\mathbf{f} = -\frac{\partial \mathbf{v}}{\partial \mathbf{x}} \mathbf{v} + O(\varepsilon)$ applied to the vector field (1.2) yields

$$\mathbf{f} = \left(\frac{1}{2} \sin 2x + a \cos x \cos y - b \sin x \sin y, \frac{1}{2} \sin 2y + a \sin x \sin y - b \cos x \cos y \right) + O(\varepsilon). \quad (\text{C.3})$$

We will also often use a formula for the divergence of this vector field:

$$\operatorname{div} \mathbf{f} = \cos 2x + \cos 2y + O(\varepsilon) = 2 \cos(x+y) \cos(y-x) + O(\varepsilon). \quad (\text{C.4})$$

Notably, the divergence does not depend on the parameters a and b .

Appendix D Properties of the rotation number

In this appendix, we prove the statement of Remark 3.4 and Lemma 4.1.

Proof of Lemma 3.4. Recall that we are assuming that the initial point \tilde{z}_0 has infinite future orbit. A standard fact on monotone degree one circle maps (possibly undefined at some points like the map P) is that there is $\rho \in \mathbb{R}$ such that the sequence $\tilde{P}^n(\tilde{z}_0) - \rho n$ is bounded. Indeed, set $a_n = \tilde{P}^n(\tilde{z}_0) - \tilde{z}_0$. Then $a_m + a_n - 1 < a_{n+m} < a_m + a_n - 1$ for any $m, n \in \mathbb{N}$: $a_{n+m} = a_n + (\tilde{P}^{m+n}(\tilde{z}_0) - \tilde{P}^n(\tilde{z}_0))$, and the second term differs from a_m by less than one due to monotonicity and degree one. This inequality implies that there is ρ such that $\rho n - 1 < a_n < \rho n + 1$ by [42, Exercise 99].

The fact above implies that ρ exists, and $\tilde{P}^n(\tilde{z}_0) = \rho n + O(1)$. Let us enumerate all intersections of the positive orbit $\mathbf{x}(t)$ of \mathbf{x}_0 with the lift of the transversal \tilde{T} as \mathbf{x}_n , treating \mathbf{x}_0 as the zeroth intersection. Then $z(\mathbf{x}_n) = \rho n + O(1)$ and $x(\mathbf{x}_n) = \pi n + O(1)$. So, $y(\mathbf{x}_n) = 2\pi z(\mathbf{x}_n) + x(\mathbf{x}_n) = (2\rho + 1)\pi n + O(1)$. Hence, the intersections of $\mathbf{x}(t)$ with \tilde{T} are at a finite distance from the ray starting at \mathbf{x}_0 with the slope $2\rho + 1$. Finally, let γ be the piece of $\mathbf{x}(t)$ between \mathbf{x}_0 and \mathbf{x}_1 , let R be the curvilinear rectangle form by γ , γ shifted up by 2π , and vertical segments connecting the endpoints of these two curves. Then, each fragment of $\mathbf{x}(t)$ between two consecutive intersections with \tilde{T} can be covered by a shift (3.3) of R and so has a bounded diameter. Hence, the whole $\mathbf{x}(t)$ lies within bounded distance from the ray above. \square

Proof of Lemma 4.1. The first two properties can be proved using the standard argument for the case of circle homeomorphisms (as written in [43, Appendix, Lemma 3]) with minor modifications. Let us now prove Property 3. Clearly, $\rho(s)$ is nondecreasing. The claim that $\rho(s)$ cannot be constant and irrational on any interval follows from Corollary 4.3.

The following auxiliary statement is needed to prove Property 4.

Lemma D.1. $\rho(s) = \frac{p}{q} \in \mathbb{Q}$ if and only if for some flat spot I_j we have $\tilde{f}^q(I_j) \in I_j + p$.

Proof. The "if" part is clear: the point $f^q(I_j)$ is periodic, so that for this point the rotation number is p/q . To prove the "only if" part, consider the map $\tilde{g}(x) = \tilde{f}^q(x) - p$. As $\rho(\tilde{f}) = p/q$, we have $\rho(\tilde{g}) = 0$. Thus, \tilde{g} has fixed points – otherwise, we would have either $\tilde{g}(x) > x$ for all x or $\tilde{g}(x) < x$, which would imply $\rho(\tilde{g}) > 0$

or $\rho(\tilde{g}) < 0$, respectively. In other words, the graph of $y = \tilde{g}(x)$ intersects the line $y = x$. The map \tilde{g} is a map with flat spots expanding outside them, as follows from the chain rule. It is impossible that all intersections of its graph with $y = x$ are at the expanding parts (then the graph goes from below $y = x$ to above $y = x$ and cannot go back); flat spots therefore intersect $y = x$. This gives a periodic orbit of f with the period q , and we can take any flat spot of f this orbit intersects as I_j . \square

Now we are ready to prove Property 4. The set $\{\rho^{-1}(p/q)\}$ is closed, non-empty, and connected by monotonicity and continuity of ρ . So, it can be either a closed interval, as claimed in Property 4, or a point. Let us show that this set is not just one point. Suppose $\rho(s_0) = p/q$; then for some flat spot I_j we have $\tilde{f}_{s_0}^q(I_j) \in I_j + p$. If $\tilde{f}_{s_0}^q(I_j)$ is not the right endpoint of I_j , we will have $\tilde{f}_{s_1}^q(I_j) \in I_j + p$ for some $s_1 > s_0$ near s_0 . Otherwise, $\tilde{f}_{s_0}^q(I_j)$ is not the left endpoint, and this holds for s_1 close to s_0 and smaller than s_0 . \square

Appendix E Perturbed flow

In this appendix, we establish several statements on the perturbed flow (3.2) used above: the first part of Proposition 3.2 and Lemmas 5.1, 5.2, and 5.3. For brevity, we will refer to the two branches of the invariant manifold of a saddle as *separatrices* throughout this appendix. Accordingly, in our notation, each saddle has two stable separatrices and two unstable ones.

The following quantifiers apply to all statements in this appendix, and will not be stated separately:

- there exists $\gamma_0 > 0$ such that for any $a_0, b_0 \in (0, \gamma_0)$ there exists $\varepsilon_1 > 0$ depending on a and b such that the statement holds for any a, b, ε with $0 < \varepsilon < \varepsilon_1$ and $|a - a_0|, |b - b_0| < \varepsilon_1$.

A compactness argument shows that ε_1 can be taken uniformly if a, b are in a fixed compact subinterval of $(0, \gamma_0)$, such as $[\delta, \gamma_0 - \delta]$ for any δ . So, Proposition 3.2 and Lemmas 5.1, 5.2, and 5.3 as stated in the main part of the paper follow from the same statements proved in the common assumptions of this Appendix.

Typically, it suffices to take $\gamma_0 = 0.1$, thus implying $0 < a, b < 0.1$ after taking small enough ε_1 . We will implicitly assume $\gamma_0 = 0.1$ throughout the Appendix. However, sometimes we are only able to prove that γ_0 exists without an explicit estimate, in which case we will write “for small enough a and b ”.

E.1 Repulsion from the cell centers

Roughly speaking, trajectories of the perturbed system (3.2) starting inside a homoclinic loop of the unperturbed system (2.1) spiral away from a fixed point near the center of the loop towards the neighborhood of the heteroclinic loop of the unperturbed system. In this subappendix, we state a lemma that formalizes this intuition and then derive several corollaries used later to describe the phase portrait of the perturbed system; we also prove the first part of Proposition 3.2.

Lemma E.1. *There exists a positive $\delta = \delta(a, b)$ such that the following holds. Let γ be a closed trajectory of the Hamiltonian system (2.1) or its homoclinic loop. Then,*

$$\iint_{\text{int } \gamma} \text{div } \mathbf{f} \, dx dy > \delta A(\gamma), \quad (\text{E.1})$$

where $A(\gamma)$ is the area bounded by γ .

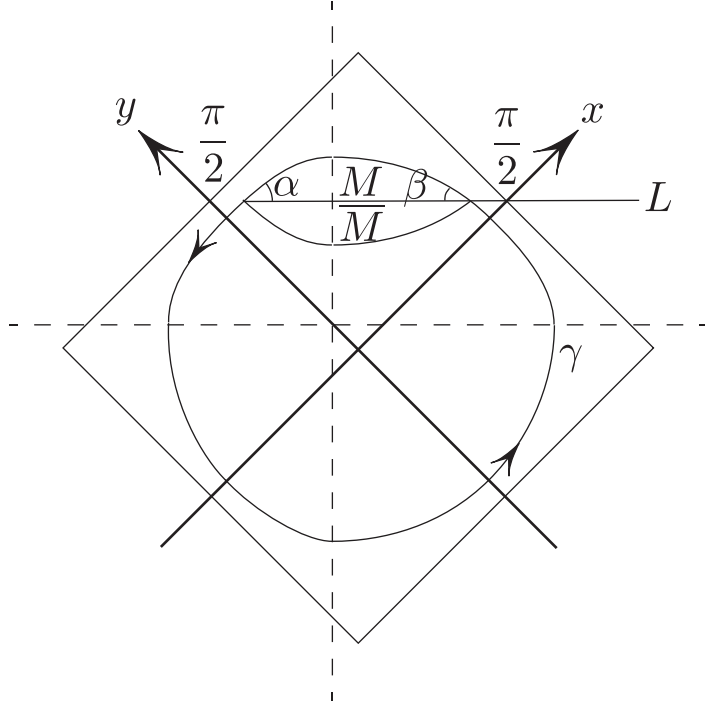


Figure 11: To the proof of Lemma E.1. For convenience, the drawing is rotated by $\pi/4$.

Proof. Let us relax the implicit assumption $0 < a_0, b_0 < 0.1$ stated in the beginning of Appendix E to $0 < |a_0|, |b_0| < 0.1$ to make the statement symmetric.

By (C.4) we have $\operatorname{div} \mathbf{f} = \psi + O(\varepsilon)$, where $\psi(x, y) = 2 \cos(x + y) \cos(y - x)$. Let us first prove that

$$\iint_{\operatorname{int} \gamma} \psi \, dx dy > 0. \quad (\text{E.2})$$

As the vertical lines $x = \frac{\pi}{2} + \pi k$ and the horizontal lines $y = \frac{\pi}{2} + \pi k$ are transversal to the flow (2.1), γ is inside one of the squares $(-\frac{\pi}{2} + \pi k_1, \frac{\pi}{2} + \pi k_1) \times (-\frac{\pi}{2} + \pi k_2, \frac{\pi}{2} + \pi k_2)$. Without loss of generality, we will assume that $\gamma \subset (-\frac{\pi}{2}, \frac{\pi}{2})^2$. Divide $\operatorname{int} \gamma$ into four parts $\operatorname{int}_1 \gamma, \dots, \operatorname{int}_4 \gamma$ lying inside each quadrant. We will prove that for each of the quadrants the integral over the corresponding part of $\operatorname{int} \gamma$ is positive, unless this part is empty. Note that in this lemma we do not require $a, b > 0$, assuming only that $a, b \neq 0$ and $|a|, |b| < 0.1$. So, the statement is symmetric, and it is enough to prove this fact for $\operatorname{int}_1 \gamma$ (and any allowed a, b):

$$\iint_{\operatorname{int}_1 \gamma} \psi \, dx dy > 0, \quad \text{provided that } \operatorname{int}_1 \gamma \text{ is non-empty.} \quad (\text{E.3})$$

We have $\operatorname{int}_1 \gamma \subset (0, \frac{\pi}{2})^2$. Denote by L the line $x + y = \frac{\pi}{2}$; this line is the diagonal of the square $(0, \frac{\pi}{2})^2$, dividing it in two parts (Figure 11), with $\psi < 0$ in the upper part and with $\psi > 0$ in the lower part. Note also that ψ is odd with respect to L (indeed, for two symmetric w.r.t. L points the values of $x - y$ are equal while the values of $\pi/2 - (x + y)$ have opposite signs). If the whole of γ is below L then ψ is positive on $\operatorname{int}_1 \gamma$, and (E.3) is clear. Along the Hamiltonian vector field (2.1), we have (using product to sum formulas)

$$\frac{d}{dt}(x + y) = \sin(x - y) + (a + b), \quad \frac{d}{dt}(x - y) = -\sin(x + y) + (b - a).$$

So, in Figure 11 the vector field (2.1) is horizontal when $\sin(y - x) = a + b$ and vertical when $\sin(x + y) = b - a$, drawn as two¹⁰ dashed lines in Figure 11. This means that in the first quadrant γ first goes (using the orientation of Figure 11) up and left, then crosses the vertical dashed line, and then goes down and left, thus it

¹⁰Those equations also give other lines, but it is easy to see that a closed trajectory remaining in $(-\frac{\pi}{2}, \frac{\pi}{2})^2$ cannot intersect them.

intersects L exactly twice (or is fully below L , this case is easy as $\psi > 0$ below L). Moreover, the angles α and β formed by the part of γ above L and the segment of L connecting two intersection points are acute. Denote by M the part of $\text{int}_1 \gamma$ above L and by \bar{M} its reflection over L . As α and β are acute, $\bar{M} \subset \text{int}_1 \gamma$. By symmetry, $\iint_{M \cup \bar{M}} \psi \, dx dy = 0$, and, as $\text{int}_1 \gamma \setminus (M \cup \bar{M})$ is below L ,

$$\iint_{\text{int}_1 \gamma} \psi \, dx dy = \iint_{\text{int}_1 \gamma \setminus (M \cup \bar{M})} \psi \, dx dy > 0.$$

Finally, taking the sum over all quadrants yields (E.2).

Let us now use (E.2) to complete the proof of the lemma. First, let us prove that for small enough δ

$$\iint_{\text{int} \gamma} \psi \, dx dy > \hat{\delta} A(\gamma).$$

Set $I(\gamma) = \iint_{\text{int} \gamma} \psi \, dx dy$. As the closed trajectories are nested, we can parametrize them by the area: $\gamma = \gamma(A)$, where $A \in [0, A_{\max}]$ with A_{\max} being the area bounded by the homoclinic loop. The function $I(A) = I(\gamma(A))$ is continuous. It is positive on $[0.001, A_{\max}]$ and thus reaches some minimum I_1 there. Then we have $I(A) \geq \frac{I_1}{A_{\max}} A$ if $A \geq 0.001$. Finally, all bounded trajectories with the area less than 0.001 lie inside the square $|x| + |y| < \frac{\pi}{2} - 0.01$ where ψ is positive and bounded away from zero by some small constant κ . So, $I(A) > \kappa A$ on $[0, 0.001]$.

It remains to note that

$$\int_{\gamma} \text{div} \mathbf{f} \, dx dy = \int_{\gamma} \psi(x, y) + O(\varepsilon) \, dx dy > 0.5 \hat{\delta} A(\gamma)$$

provided that ε is small enough. \square

Corollary E.2. *The perturbed system (3.2) has no periodic orbits or homoclinic loops inside or close to homoclinic loops of the unperturbed system.*

More formally, let L_δ denote the δ -neighborhood of the region bounded by a homoclinic loop. Then, for any $c > 0$ for all small enough ε the perturbed system (3.2) has no periodic orbits or homoclinic loops contained inside $L_{c\varepsilon}$ with smallness of ε depending on c .

Proof. Assume the contrary: there exists a periodic orbit or a homoclinic loop γ_ε of the perturbed system contained inside $L_{c\varepsilon}$. But then γ_ε is $O(\varepsilon)$ -close to a periodic orbit γ of the Hamiltonian system. By the divergence theorem, we have $\iint_{\text{int} \gamma_\varepsilon} \text{div}(\mathbf{v} + \varepsilon \mathbf{f}) \, dx dy = 0$. Since near the elliptic fixed points of the unperturbed system the divergence of the perturbation is negative by (C.4), γ_ε cannot be very small so that there exists $S > 0$ independent of ε such that the area bounded by γ is greater than S . But then

$$0 = \varepsilon^{-1} \iint_{\text{int} \gamma_\varepsilon} \text{div}(\mathbf{v} + \varepsilon \mathbf{f}) = \iint_{\text{int} \gamma_\varepsilon} \text{div} \mathbf{f} = \iint_{\text{int} \gamma} \text{div} \mathbf{f} + O(\varepsilon) > \delta S + O(\varepsilon) > 0$$

when ε is small enough. This contradiction proves the corollary. \square

Corollary E.3. *Referring to Figure 9, the homoclinic loops of the unperturbed system are split “outwards”: trajectories starting inside the former loops near the loops escape them. The size of the split, i.e., the distance between two separatrices a fixed distance away from the saddle is of order ε . Moreover, one of the two stable separatrices of each saddle never intersects the transversal T defined in Section 3.2 (as it is “trapped inside the loop” as in Figure 9).*

Proof. Consider any line segment L transversal to a homoclinic loop of the unperturbed Hamiltonian system. Let S be the segment between the intersections of the stable and unstable separatrices of the perturbed system that are continuations of the former homoclinic loop of the unperturbed system (we consider intersections closest to the saddle along the separatrices). Consider the closed contour B formed by S together with the two pieces of separatrices of perturbed system connecting the saddle with the endpoints of S (this is a standard construction called *Bendixson*

bag). Note that these separatrix pieces are $O(\varepsilon)$ -close to the homoclinic loops of the Hamiltonian system. Hence, the same argument as in the proof of Corollary E.2 shows that integral of $\operatorname{div} \mathbf{f}$ over the area bounded by B is positive and of order ε . It equals to the flux of $\mathbf{v} + \varepsilon \mathbf{f}$ through B , so this flux is also positive and of order ε . All this flux goes through S (as separatrices are integral curves of $\mathbf{v} + \varepsilon \mathbf{f}$), and restricted to S the vector field is close to a constant. Thus, this flux goes outside and the length of this segment (which measures separatrix splitting) is of order ε . To prove the "moreover" part, we note that the stable manifold is trapped inside B in backward time. \square

Corollary E.4. *The perturbed system (3.2) on the torus has four fixed points: two saddles that are continuations of the saddles of the unperturbed flow \mathbf{v} , and two unstable foci that are continuations of the two centers of \mathbf{v} .*

Proof. A straightforward computation shows that when $0 < a, b < 0.1$ the unperturbed Hamiltonian system has two saddles and two centers on the fundamental domain $[-\frac{\pi}{2}, \frac{\pi}{2}] \times [-\frac{\pi}{2}, \frac{3\pi}{2}]$; and the map $\mathbf{x} \mapsto \mathbf{v}(\mathbf{x})$ has nonzero Jacobians at these points. As the perturbation $\varepsilon \mathbf{f}$ is small in the C^1 topology, by the implicit function theorem these fixed points are smooth functions of ε near $\varepsilon = 0$, and there are no other fixed points in small neighborhoods of these points. This implies that there are no other fixed points at all for small ε , as outside the neighborhoods above $|\mathbf{v}|$ is separated from zero.

Let us now classify these four fixed points of the perturbed system. The saddles of the unperturbed system clearly remain saddles for the perturbed system as well. A straightforward computation shows that the centers of the unperturbed system are quite close to the points $(0, 0)$ and $(0, \pi)$: namely, one of them satisfies $|x| + |y| < \frac{\pi}{4}$, and the other one satisfies $|x| + |y - \pi| < \frac{\pi}{4}$. Hence, continuations of these centers for the perturbed system are in the areas where $\operatorname{div} \mathbf{f} > 0$ by (C.4). For the centers, the two eigenvalues are purely imaginary; for the perturbed system these eigenvalues are close to the ones for the unperturbed system so they are complex and conjugate to each other, and their sum is $\operatorname{div}(\mathbf{v} + \varepsilon \mathbf{f}) = \varepsilon \operatorname{div} \mathbf{f} > 0$. Hence, the real parts of both eigenvalues are positive, and centers of the unperturbed system are continued for the perturbed system as unstable foci. \square

Corollary E.5. *For the flow (3.2), the positive orbit with the starting value of $x \in [-\frac{\pi}{2}, \frac{\pi}{2})$ intersects the transversal $\{x = \frac{\pi}{2}\}$ unless the initial point is a fixed point or lies on the stable manifold of a saddle.*

Proof. Consider any trajectory γ going from $\{x = -\frac{\pi}{2}\}$ to $\{x = \frac{\pi}{2}\}$. Let U be the open set bounded by γ , γ shifted up by 2π , and the transversals $\{x = \pm\frac{\pi}{2}\}$. We can shift the initial point vertically by $2\pi k$ to be in this domain, denote this shifted point by \mathbf{x} . As the x -component of the vector field is positive on both vertical transversals, the positive orbit of \mathbf{x} can only escape U through $\{x = \frac{\pi}{2}\}$. Suppose this does not happen, then the orbit stays in U . By the Poincaré-Bendixson Theorem the ω -limit set of \mathbf{x} either is (1) a periodic orbit, (2) a fixed point, or (3) a union of fixed points, homoclinic, or heteroclinic orbits.

We claim that there are no periodic orbits contained in U . Indeed, for a large enough c , any orbit that is outside homoclinic loops of the unperturbed system and stays $c\varepsilon$ -far from these loops reaches $\{x = \frac{\pi}{2}\}$, as the orbit of the same initial point for the unperturbed system reaches this transversal, and the orbit for perturbed system stays $O(\varepsilon)$ -close to it. If the orbit is inside the loops or is $c\varepsilon$ -close to them, it cannot be periodic by Corollary E.2.

Now, consider cases 2 and 3, when $\omega(\mathbf{x})$ contains a fixed point. The fixed points of the perturbed system are described by Corollary E.4 (note that U is a fundamental domain). Assume \mathbf{x} is not one of those fixed points. Then unstable foci cannot be in the ω -limit set, and the only possibility left is that $\omega(\mathbf{x})$ contains a saddle. Then either \mathbf{x} is on a stable manifold of the saddle, which finishes the proof, or $\omega(\mathbf{x})$ contains one of the unstable separatrices of the saddle as well, moving us to case (3). In case 3, only homoclinic or heteroclinic orbits connecting saddles are relevant, as unstable foci cannot belong to $\omega(\mathbf{x})$. We claim that there are no such orbits contained in U . Homoclinic saddle loops are forbidden by Corollary E.2. Heteroclinic saddle connections between the two saddles in U are forbidden by for

the following reason: when $\varepsilon = 0$, there is a trajectory of \mathbf{v} going from $x = -\frac{\pi}{2}$ to $x = \frac{\pi}{2}$ and separating the two saddles of \mathbf{v} by Lemma B.2; this trajectory survives for the perturbed system when ε is small enough and hence it prohibits heteroclinic connection between the two saddles in U . Hence, the orbit of any point that is not a fixed point and does not lie on a stable separatrix leaves U via its right side $x = \frac{\pi}{2}$. \square

E.2 Phase portrait of the perturbed flow

In this subappendix, we prove the first part of Proposition 3.2. We refer to the system with $a = a_0$, $b = b_0$ (recall the discussion in the beginning of Appendix E), and $\varepsilon = 0$ as the *unperturbed system* and the system with the parameters a , b , and ε satisfying $|a - a_0|, |b - b_0|, 0 < \varepsilon < \varepsilon_1$ the *perturbed system*.

Proof of the first part of Proposition 3.2. There are two saddles, two sources, and no other fixed points. A straightforward computation shows that when $0 < a_0, b_0 < 0.1$, the unperturbed Hamiltonian system has two saddles and two centers on $[-\frac{\pi}{2}, \frac{\pi}{2}] \times [-\frac{\pi}{2}, \frac{3\pi}{2}]$; and the map $\mathbf{x} \mapsto \mathbf{v}(\mathbf{x})$ has nonzero Jacobians at these points. As the perturbation $\varepsilon \mathbf{f} + (b - b_0, a - a_0)$ is $O(\varepsilon_1)$ -small in the C^1 topology, by the implicit function theorem these fixed points are smooth functions of a , b , and ε near $a = a_0$, $b = b_0$, $\varepsilon = 0$, and there are no other fixed points in small neighborhoods of these points. This implies that there are no other fixed points at all when the parameters are close enough to $(a_0, b_0, 0)$, as outside the neighborhoods above $|\mathbf{v}|$ is separated from zero.

Let us now classify these four fixed points of the perturbed system. The saddles of the unperturbed system clearly remain saddles for the perturbed system as well. A straightforward computation shows that one of centers of the unperturbed system satisfies $|x| + |y| < \frac{\pi}{4}$, while the other satisfies $|x| + |y - \pi| < \frac{\pi}{4}$; and $\operatorname{div} \mathbf{f} > 0$ in both of these regions by (C.4). For the centers, the two eigenvalues are purely imaginary; for the perturbed system these eigenvalues are complex conjugate to each other and with positive real parts since $\operatorname{div}(\mathbf{v} + \varepsilon \mathbf{f}) > 0$ as $\operatorname{div} \mathbf{v} = 0$. Thus centers of the unperturbed system become unstable foci of the perturbed system.

The forward trajectory of any point that is not on a stable manifold of a saddle and is not one of the sources intersects the transversal T . This is the conclusion of Corollary E.5 proved above.

The reverse-time first return map is defined and continuous on the whole circle T except for two closed intervals I_1, I_2 . Each of these intervals is bounded by an intersection of the two unstable manifolds of a saddle with T . One-sided limits of this map at the endpoints of such interval I_j exist, and both coincide with the point b_j of intersection of the stable manifold of the same saddle with T .

Recall T is the vertical segment $x = -\frac{\pi}{2}$, the lift of a circle on the torus. By Corollary E.3, one of the two stable separatrices of each saddle never intersects T . Consider the forward-time first return map P first. By Corollary E.5, it is defined on the whole of T except for the two points of intersection of the stable manifolds of the two saddles with T . Since these intersections are transversal for the unperturbed system, they persist for the perturbed system if ε_1 is small enough. Consider one of the saddles and the corresponding coordinate $y = b_i$ on the transversal where P is undefined. Both unstable separatrices of this saddle intersect T (they cannot coincide with a stable separatrix of another saddle as shown in the proof of Corollary E.5). This means that left and right limits of P at b_i exist and are given by the intersections of the two unstable manifolds of the saddle with T .

Referring to Figure 9, let b_1 and b_2 be the y -coordinates of the two points where P is undefined and let I_1 be the closed arcs whose ends are the left and the right limits of P at b_1 , with I_2 defined similarly. As P is smooth on $S^1 \setminus \{b_1, b_2\}$, the inverse map Q exists on $S^1 \setminus (I_1 \cup I_2)$. Moreover, one-sided limits at the endpoints of I_i exist and are equal to b_i . Hence, setting $Q|_{I_i} = b_i$ turns Q into a continuous map with two flat spots. \square

E.3 Monotonicity of the flat spots heights

In this subappendix, we prove Lemma 5.2. To this end, it is enough to prove the estimate on the derivative claimed in Lemma 5.2 in the quantifiers stated in the beginning of Appendix E. The lemma will follow by compactness as discussed in beginning of Appendix E.

Proof of Lemma 5.2. Recall that "flat spots heights" $\tilde{b}_j(a, b, \varepsilon)$ were defined as the values of $z = \frac{y-x}{2\pi}$ at the lifts to \mathbb{R} of the images of the flat spots under the map Q_s , Figure 9); "flat spots heights" \tilde{b}_j are the y -coordinates of the intersections of stable manifolds of the two saddles with the transversal.

When $\varepsilon = 0$, for any fixed $a_0, b_0 \in (0, 0.1)$ the functions \tilde{b}_1, \tilde{b}_2 are defined by Lemma B.2, and Lemma B.3 claims that $\frac{\partial \tilde{b}_j}{\partial a} < -\frac{1}{2\pi}$ – here we need to divide by 2π because Lemma B.3 used y as the coordinate on the transversal instead of z . As the separatrices smoothly depend on the parameters and intersect the transversal transversally, \tilde{b}_1 and \tilde{b}_2 are actually defined and C^∞ -smooth on some small neighborhood of $(a_0, b_0, 0)$ – even allowing ε to be negative. As $\frac{\partial \tilde{b}_j}{\partial a}$ is continuous at $(a_0, b_0, 0)$, we have the weaker estimate $\frac{\partial \tilde{b}_j}{\partial a} < -0.15$ (note that $0.15 < \frac{1}{2\pi}$) for any a and b with $|a - a_0|, |b - b_0| < \varepsilon_1$ and any positive $\varepsilon < \varepsilon_1$ when ε_1 is small enough. \square

E.4 Contraction property of the first return map

Before proving that the first return map is contracting, we state a general fact relating the derivative of a first return map with the divergence of the vector field. Consider a C^1 vector field $v(x)$ on \mathbb{R}^2 . Let $x(t)$, $t \in [t_1, t_2]$ be its trajectory. Denote $x_1 = x(t_1)$, $x_2 = x(t_2)$.

We need the following well known ([44, §27.6]) fact.

Lemma E.6 (Liouville's Theorem). *Let ψ be the time $t_2 - t_1$ flow of v . Then*

$$\det D_{x_1} \psi = \exp \left(\int_{t_1}^{t_2} \operatorname{div} v \, dt \right). \quad (\text{E.4})$$

Corollary E.7. *Consider a transversal T_1 passing through x_1 and a transversal T_2 passing through x_2 . Let s_1 and s_2 be natural (arc length) parameters on T_1 and T_2 that are zero at x_1 and x_2 . Let $v_{n,1}, v_{n,2} > 0$ be the components of $v(x_1), v(x_2)$ normal to T_1, T_2 . Let $h : T_1 \mapsto T_2$ be the Poincaré map (we assume that the orientation of T_1 and T_2 is chosen so that h is increasing). Then*

$$h'(0) = \frac{v_{n,1}}{v_{n,2}} \exp \left(\int_{t_1}^{t_2} \operatorname{div} v \, dt \right). \quad (\text{E.5})$$

Informal proof. Consider stationary flow of compressible fluid with velocity field v . Let $\Delta I_1 \subset T_1$ be a small interval covering x_1 , let $\Delta I_2 = h(\Delta I_1)$. Denote by \mathcal{T} the corresponding trajectory tube between ΔI_1 and ΔI_2 .

Take some small time Δt . During this time, the volume flowing into \mathcal{T} will be $\Delta V_1 = \Delta t \cdot v_{n,1} |\Delta I_1|$, and the volume flowing out of \mathcal{T} will be $\Delta V_2 = \Delta t \cdot v_{n,2} |\Delta I_2|$. Small volume ΔV of liquid entering \mathcal{T} exits it having the volume $J \Delta V$, where

$$J = \exp \left(\int_{t_1}^{t_2} \operatorname{div} v \, dt \right),$$

due to Lemma E.6. Thus, the outgoing volume is J times the incoming volume:

$$\Delta V_2 = J \Delta V_1, \quad \text{or} \quad \Delta t \cdot v_{n,2} |\Delta I_2| = J \Delta t \cdot v_{n,1} |\Delta I_1|.$$

This yields

$$h'(0) = \frac{|\Delta I_2|}{|\Delta I_1|} = J \frac{v_{n,1}}{v_{n,2}}.$$

\square

Formal proof. Recall that ψ denotes the time $t_2 - t_1$ flow, $\psi(x_1) = x_2$, and $D_{x_1}\psi : T_{x_1}\mathbb{R}^2 \mapsto T_{x_2}\mathbb{R}^2$ denotes the differential of ψ at x_1 . Let us pick the basis of T_{x_1} consisting of the vector $u_1 = v(x_1)/v_{n,1}$ and of $u_2 =$ a unit vector tangent to T_1 chosen so that the basis is right-handed. We pick the basis w_1, w_2 in T_{x_2} in the same way. Note that $\det([u_1, u_2]) = 1$ and $\det([w_1, w_2]) = 1$. This means that the determinant of $D_{x_1}\psi$ written in these bases will be

$$J = \exp\left(\int_{t_1}^{t_2} \operatorname{div} v \, dt\right)$$

by Lemma E.6. As $D_{x_1}\psi$ maps $v(x_1)$ into $v(x_2)$, it maps $u_1 = v(x_1)/v_{n,1}$ into $\frac{v_{n,2}}{v_{n,1}}w_1$. As $\det(D_{x_1}\psi) = J$, this means

$$D_{x_1}\psi = \begin{pmatrix} \frac{v_{n,2}}{v_{n,1}} & * \\ 0 & \frac{Jv_{n,1}}{v_{n,2}} \end{pmatrix}.$$

Now, let $\phi : T_1 \mapsto \mathbb{R}^2$ be the embedding and let $\pi : \mathbb{R}^2 \mapsto T_2$ be the projection onto T_2 along the trajectories of v . Using the bases in T_{x_1} and T_{x_2} chosen above, we have

$$D_0\phi : \mathbb{R} \mapsto T_{x_1} = \begin{pmatrix} 0 \\ 1 \end{pmatrix}, \quad D_{x_2}\pi : T_{x_2} \mapsto \mathbb{R} = (0 \ 1).$$

We can write the Poincaré map as $h = \pi \circ \psi \circ \phi$, and

$$h' = D_{x_2}\pi \cdot D_{x_1}\psi \cdot D_0\phi = \frac{Jv_{n,1}}{v_{n,2}}.$$

□

Next, let us prove a lemma describing the integral of the divergence along trajectories realizing the Poincaré map for our particular system (3.2). As $\operatorname{div} \mathbf{v} = 0$, this divergence is $\varepsilon \operatorname{div} \mathbf{f}$.

Lemma E.8. *For small enough a and b the following holds for all small enough ε . Consider a solution of (3.2) starting at $t = t_0$ on the transversal T defined in Section 3.2, and let t_1 be the time of first return to T . Then*

$$\int_{t_0}^{t_1} \operatorname{div} \mathbf{f} \, dt < -C_d |\ln b| < 0, \quad (\text{E.6})$$

where the integral is taken along the solution, and the positive constant C_d does not depend on ε , chosen initial data on T and the parameters a and b .

Proof. First, we need to establish the estimate

$$t_1 - t_0 > |\ln b|.$$

Consider solution of (3.2) starting on T (more precisely, on its lift to \mathbb{R}^2) with $x = -\frac{\pi}{2}$. Set $w(t) = x(t) + \frac{\pi}{2}$, where $x(t)$ is the first coordinate of this solution. By (2.1) we have

$$\dot{w} = -\cos\left(w - \frac{\pi}{2}\right) \sin(y) + b + O(\varepsilon) < \left|\cos\left(w - \frac{\pi}{2}\right)\right| + \frac{b}{2} < w + \frac{b}{2}.$$

We have $w(t_0) = 0$; the corresponding solution of $\dot{w} = w + \frac{b}{2}$ is $w(t) = \frac{b}{2}(e^{t-t_0} - 1)$. Solution of (3.2) returns to T when $w = \pi$. This gives

$$t_1 - t_0 > \ln(2\pi/b + 1) > \ln(1/b) = |\ln b|.$$

Getting back to estimating the integral of the divergence, we will use formula (C.4):

$$\operatorname{div} \mathbf{f} = \cos(2x) + \cos(2y) + O(\varepsilon) = 2 \cos(x+y) \cos(y-x) + O(\varepsilon).$$

The leading term $2 \cos(x+y) \cos(y-x)$ is π -periodic, positive in the squares surrounding cell centers with the vertices at the midpoints of the sides of the cell (for

the cell $[-\frac{\pi}{2}, \frac{\pi}{2}]^2$ this square is $\{|x| + |y| < \frac{\pi}{2}\}$, and negative outside these squares. Let us call the squares where $2 \cos(x+y) \cos(y-x)$ is positive *central squares*. We will use that a and b are small enough – as assumed in the beginning of Appendix E, we have $a, b < \gamma_0$ with γ_0 as small as needed. Then trajectories whose backward orbit is captured inside the former separatrix loops of the unperturbed system occupy most of the central squares, and only their corners of size $O(\gamma_0)$ can intersect trajectories of the perturbed system that realize Poincaré map. These corners are crossed during the time $O(\gamma_0)$; for the rest of the time the divergence is negative, and at least half of that time the divergence is bounded away from zero. Hence, the time average of the divergence is bounded from above by a negative constant; together with the estimate on the time $t_1 - t_0$ this gives (E.6). \square

Now, we are ready to prove the contraction of the first return map.

Proof of Lemma 5.1. We use the formula (E.5) for the derivative of P applied to the vector field $v = \mathbf{v} + \varepsilon \mathbf{f}$. As this formula uses natural parameter on the transversal, it can be applied to P written using the coordinate y , which we denote \hat{P} . In (E.5), we have $\frac{v_{n,1}}{v_{n,2}} < 1 + 3\varepsilon$: restricted to the transversal T where $x = \frac{\pi}{2} + \pi k$, the normal component of \mathbf{v} is b and the normal component of $\varepsilon \mathbf{f}$ is $-\varepsilon b \sin(x) \sin(y)$ by (C.3), which is bounded by εb . As $\text{div } \mathbf{v} = 0$, the divergence of v is $\varepsilon \text{div } \mathbf{f}$, and we get

$$\frac{d}{dz} P = \frac{d}{dy} \hat{P} < (1 + 3\varepsilon) \exp\left(\varepsilon \int_{t_1}^{t_2} \text{div } \mathbf{f} dt\right),$$

where the integral is along the trajectory of (3.2) connecting y with $P(y)$. The integral is bounded from above by $-C_d |\ln b|$ according to Lemma E.8, so we get

$$\frac{d}{dz} P < (1 + 3\varepsilon) \exp(1 - \varepsilon C_d |\ln b|) < (1 + 3\varepsilon)(1 - 0.5\varepsilon C_d |\ln b|) < 1 - \varepsilon,$$

as b is small enough. \square

Remark E.9. *The derivative of the inverse-time Poincaré map Q has infinite singularities at the boundaries of each flat spot.*

Proof. The jumps of the forward-time Poincaré map P happen at the points b_1 and b_2 (Figure 9) where stable manifolds of the two saddles intersect the transversal. When the starting point on the transversal approaches b_1 or b_2 , the time spent near the corresponding saddle goes to infinity, and the integral (E.6) goes to $-\infty$ as the divergence is negative near both saddles. So, proof of Lemma 5.1 implies that the derivative of P has zero limit at the jump singularities. For its inverse Q , this means the derivative has infinite singularities at the boundaries of the flat spots. \square

E.5 Monotonicity with respect to the parameter

In this appendix, we prove Lemma 5.3. Throughout this subappendix, we will assume that b is fixed; with a variable, we need a notation that reflects the dependence of the vector field on a . To that end we denote by \mathbf{w}_a the vector field in the RHS of (3.2) with given a , writing $\mathbf{w}_a = \mathbf{v}_a + \varepsilon \mathbf{f}_a$.

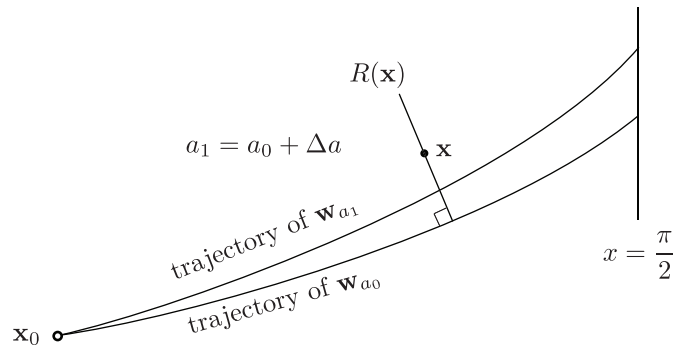


Figure 12: A tube.

Let us now introduce a technical notion of *tube* (Figure 12) that we use to compare trajectories of \mathbf{w}_a with different values of a . To specify a tube, we fix some a_0 , an initial point $\mathbf{x}_0 = (x_0, y_0)$ with $x_0 \in [-\pi/2, \pi/2)$, and Δa . We always assume that Δa is small enough, depending on \mathbf{x}_0 . We also assume that \mathbf{x}_0 is such that its positive \mathbf{w}_{a_0} -orbit intersects the line $\{x = \pi/2\}$. Denote the trajectory of \mathbf{x}_0 by l_0 . For a point \mathbf{x} close to l_0 , denote by $R(\mathbf{x})$ the perpendicular to l_0 passing through \mathbf{x} . For small enough Δa denote $a_1 = a_0 + \Delta a$, $\mathbf{w}_0 = \mathbf{w}_{a_0}$ and $\mathbf{w}_1 = \mathbf{w}_{a_1}$. Let l_1 be the trajectory of \mathbf{w}_1 starting at \mathbf{x}_0 ; this trajectory reaches $\{x = \pi/2\}$ as well if Δa is sufficiently small. Let \mathcal{T} be the *tube* bounded by l_0 , l_1 , and the segment of the line $\{x = \pi/2\}$ between l_0 and l_1 . Note that l_0 and l_1 may intersect at some points other than \mathbf{x}_0 (the figure does not show such a case).

We assume that Δa is so small that

$$\text{for any } \mathbf{x} \in \mathcal{T}, \text{ the angle between } \mathbf{w}_0(\mathbf{x}) \text{ and } R(\mathbf{x}) \text{ is in } [\pi/2 - 0.01, \pi/2 + 0.01]. \quad (\text{E.7})$$

Lemma E.10. *The lengths of all trajectories of (3.2) realizing the Poincaré map from $x = -\frac{\pi}{2}$ to $\frac{\pi}{2}$ are bounded (uniformly over all trajectories).*

Proof. Let $l(y)$ be the length of such a trajectory starting at $(-\pi/2, y)$. This function is continuous on the whole circle except the points b_1 and b_2 (Figure 9), and at these two points it has one-sided limits equal to the lengths of the "limit" paths along separatrices. Hence, $l(y)$ is bounded. \square

Let $R_{\mathcal{T}}(x) = R(x) \cap \mathcal{T}$.

Lemma E.11. *There exists $c > 0$ such that, given any tube \mathcal{T} and $x \in l_0$, the flux of \mathbf{w}_0 through $R_{\mathcal{T}}(x) = R(x) \cap \mathcal{T}$ is bounded by $c\Delta a$.*

Proof. Let s be the natural parameter on l_0 with $s = 0$ corresponding to \mathbf{x}_0 , and let $\phi(s)$ be the flux of \mathbf{w}_0 through $R_{\mathcal{T}}(x)$, where $x \in l_0$ is given by s . Note that $\phi \geq 0$ by (E.7). Let us show that

$$\frac{\partial}{\partial s} \phi \leq c_1(|\Delta a| + \phi) \quad (\text{E.8})$$

for some (uniform) constant c_1 . This will imply the lemma because $\phi(0) = 0$ and the lengths of trajectories l_0 starting with $x \in (-\pi/2, \pi/2)$ and crossing $\{x = \pi/2\}$ are uniformly bounded by Lemma E.10. Indeed, for $\tilde{\phi} = \phi/|\Delta a|$ equation E.8 implies $\frac{\partial}{\partial s} \tilde{\phi} \leq c_1(1 + \tilde{\phi})$, so $\tilde{\phi} = O(1)$ and $\phi = O(\Delta a)$.

To prove (E.8), we take small Δs and consider the part of \mathcal{T} between $R_{\mathcal{T}}(s)$ and $R_{\mathcal{T}}(s + \Delta s)$. Let us apply the divergence theorem to the flux of \mathbf{w}_0 through the boundary of this domain. The flux through the l_0 side is zero. The flux of \mathbf{w}_1 through the l_1 side is zero, and so the flux of $\mathbf{w}_0 = \mathbf{w}_1 + O(\Delta a)$ is $O(\Delta a \Delta s)$. According to the divergence theorem we then have $\phi(s + \Delta s) - \phi(s) + O(\Delta a \Delta s) = \iint \text{div } \mathbf{w}_0$.

Consider now small neighborhoods of the saddles where $\text{div } \mathbf{w}_0$ is negative according to (C.4). In these neighborhoods the divergence theorem gives $\frac{\partial}{\partial s} \phi < O(\Delta a)$, which implies (E.8). Outside these neighborhoods we claim that the width of \mathcal{T} is $O(\phi)$. This is because $|\mathbf{w}_0|$ is separated from zero and its angle with the two sides of the rectangle formed by transversals is close to the right angle, so that the flux ϕ through $R_{\mathcal{T}}$ is of the same order as the width of \mathcal{T} . Thus, the area of the part of \mathcal{T} in question is $O(\phi \Delta s)$, and $\iint \text{div } \mathbf{w}_0 = O(\phi \Delta s)$, giving (E.8). \square

Given a tube, let \mathbf{x}'_0 and \mathbf{x}'_1 be the intersections of l_0 and l_1 with $\{x = \pi/2\}$. Let $\Delta H_0 = H_{a_0}(\mathbf{x}'_0) - H_{a_0}(\mathbf{x}_0)$ and $\Delta H_1 = H_{a_1}(\mathbf{x}'_1) - H_{a_1}(\mathbf{x}_0)$.

Lemma E.12.

$$y(\mathbf{x}'_1) - y(\mathbf{x}'_0) = \Delta a \frac{\pi/2 - x(\mathbf{x}_0)}{b} + O(\Delta H_1 - \Delta H_0).$$

Proof. Set $H_0 = H_{a_0}(\mathbf{x}_0)$ and $H_1 = H_{a_1}(\mathbf{x}_0)$. We have $H_1 - H_0 = -x(\mathbf{x}_0)\Delta a$. Set $H'_0 = H_{a_0}(\mathbf{x}'_0) = H_0 + \Delta H_0$ and $H'_1 = H_{a_1}(\mathbf{x}'_1) = H_1 + \Delta H_1$. We have $H'_1 - H'_0 = -\frac{\pi}{2}\Delta a + b(y(\mathbf{x}'_1) - y(\mathbf{x}'_0))$. Thus,

$$b(y(\mathbf{x}'_1) - y(\mathbf{x}'_0)) = H'_1 - H'_0 + \frac{\pi}{2}\Delta a = -x(\mathbf{x}_0)\Delta a + (\Delta H_1 - \Delta H_0) + \frac{\pi}{2}\Delta a.$$

□

Lemma E.13. ΔH_0 is the flux of $\varepsilon \mathbf{f}_{a_0}$ through l_0 . Similarly, ΔH_1 is the flux of $\varepsilon \mathbf{f}_{a_1}$ through l_1 .

Proof. Set $\mathbf{f} = \mathbf{f}_{a_i}$, $\mathbf{w} = \mathbf{w}_i$, $\Delta H = \Delta H_i$, and $l = l_i$, where $i = 0, 1$. The flux of $\varepsilon \mathbf{f}$ through l is $\int_l \langle \varepsilon \mathbf{f}(t), -J(\mathbf{w})dt \rangle$, where t is the time, $\langle \cdot, \cdot \rangle$ is the inner product, and J is the rotation by $-\pi/2$. Using $\mathbf{w} = J\nabla H + \varepsilon \mathbf{f}$ we have

$$\int_l \langle \varepsilon \mathbf{f}, -J(J\nabla H + \varepsilon \mathbf{f}) \rangle dt = \underbrace{\int_l \langle \varepsilon \mathbf{f}, -J^2 \nabla H \rangle dt}_{\int_l \langle \nabla H, \varepsilon \mathbf{f} \rangle dt} - \underbrace{\int_l \langle \varepsilon \mathbf{f}, J(\varepsilon \mathbf{f}) \rangle dt}_{=0} = \int_l \dot{H} dt = \Delta H.$$

□

Remark E.14. Together with Lemma E.10, Lemma E.13 implies that the change of H along a trajectory of (3.2) defining the Poincaré map is $O(\varepsilon)$.

Lemma E.15.

$$\Delta H_1 - \Delta H_0 = \iint_{\mathcal{T}} \varepsilon \operatorname{div} \mathbf{f}_{a_0} + O(\varepsilon \Delta a).$$

Here, the integral over the parts of \mathcal{T} with l_0 above l_1 are included with positive sign, and over the parts with l_0 below l_1 have negative sign.

Proof. This is the divergence theorem applied to the flux of $\varepsilon \mathbf{f}_{a_0}$ through the boundary of \mathcal{T} . To be more precise, consider a contour formed by l_1 oriented forward, followed by the vertical segment connecting \mathbf{x}'_1 with \mathbf{x}'_0 , and then completed by l_0 oriented backward. Applying the divergence theorem, we get that the integral of the divergence (with appropriate signs for different parts of \mathcal{T}) is equal to the sum of three fluxes: flux through l_1 , flux through the vertical segment, and the flux through l_0 oriented backward. The last one is equal to $-\Delta H_0$ by Lemma E.13. Since $\mathbf{f}_{a_1} = \mathbf{f}_{a_0} + O(\Delta a)$ because $\mathbf{f} = \mathbf{f}(x, y, a, b, \varepsilon)$ is C^1 -smooth by Proposition 3.1, the flux through l_1 is $\Delta H_1 + O(\varepsilon \Delta a)$. By Lemma E.11 together with the fact that near the line $x = \frac{\pi}{2}$ the vector field \mathbf{w}_0 is close to (b, a) , the length of the vertical segment connecting \mathbf{x}'_0 with \mathbf{x}'_1 is $O(\Delta a)$. Thus, the flux of $\varepsilon \mathbf{f}_{a_0}$ through this segment is $O(\varepsilon \Delta a)$. This completes the proof of the lemma. □

Lemma E.16. For any $C_1 > 0$ there exists $C_2 > 0$ such that the following holds. If the distance between l_0 and the saddles of \mathbf{w}_0 is greater than $C_1 \varepsilon$, then

$$|\Delta H_1 - \Delta H_0| < C_2 \sqrt{\varepsilon} \Delta a.$$

Proof. By Lemma E.15 it is enough to show that $\iint_{\mathcal{T}} \operatorname{div} \mathbf{f}_{a_0} = O(\Delta a / \sqrt{\varepsilon})$, or, that the area of \mathcal{T} is bounded by $O(\Delta a / \sqrt{\varepsilon})$. Let U_1 be the (possibly empty) part of \mathcal{T} that is $\sqrt{\varepsilon}$ -close to saddles, and set $U_2 = \mathcal{T} \setminus U_1$. The length of the vector field \mathbf{w}_0 is bounded from below (up to a multiplicative constant) by $\sqrt{\varepsilon}$ in U_2 , and by ε in U_1 . Thus, by Lemma E.11 and (E.7) the width of \mathcal{T} is $O(\Delta a / \varepsilon)$ in U_1 , and $O(\Delta a / \sqrt{\varepsilon})$ in U_2 . As the length of U_1 is $O(\sqrt{\varepsilon})$, this means that the areas of U_1 and U_2 are both bounded by $O(\Delta a / \sqrt{\varepsilon})$, as needed. □

Let $\hat{P}(y)$ be the Poincaré map from the transversal $x = -\pi/2$ to the transversal $x = \pi/2$ written using the y coordinate. Note that $\hat{P}(y)$ is not to be confused with \tilde{P} whose argument is $z = \frac{y-x}{2\pi}$ (in Section 3.2) rather than y .

Corollary E.17. For any $C_1 > 0$ there exists $C_2 > 0$ such that the following holds. If y is such that the trajectory connecting $(-\frac{\pi}{2}, y)$ with $(\frac{\pi}{2}, \hat{P}(y))$ is $C_1 \varepsilon$ -far from the saddles, then

$$\frac{\partial}{\partial a} \hat{P}(y) = \frac{\pi}{b} + O(\sqrt{\varepsilon}) > 0$$

with $|O(\sqrt{\varepsilon})| < C_2 \sqrt{\varepsilon}$.

Proof. Consider a tube starting at $\mathbf{x}_0 = (-\pi/2, y)$. We have

$$\frac{\partial}{\partial a} \hat{P}(y) = \lim_{\Delta a \rightarrow 0} \frac{y(\mathbf{x}'_1) - y(\mathbf{x}'_0)}{\Delta a}.$$

By Lemma E.12 $\frac{y(\mathbf{x}'_1) - y(\mathbf{x}'_0)}{\Delta a} = \frac{\pi}{b} + O(|\Delta H_1 - \Delta H_0|/\Delta a)$. By Lemma E.16 this gives the required estimate. \square

The argument above implies monotonicity of the Poincaré map far from its discontinuities which correspond to the trajectories bumping into the saddles. Let us continue with another argument showing monotonicity near the discontinuity points.

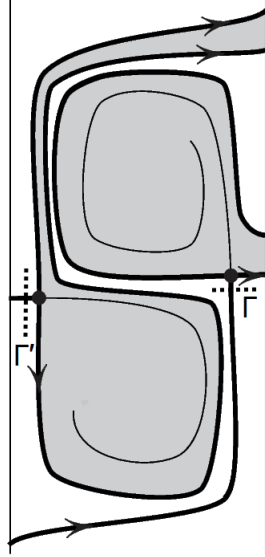


Figure 13: Transversals (dashed) used to study trajectories passing near saddles.

Lemma E.18. *There exist $C_1, C_2 > 0$ such that the following holds. Consider a tube starting at a point \mathbf{x}_0 that is $C_1\varepsilon$ -close to a saddle and lies on one of the transversals Γ or Γ' (Figure 13). Then*

$$|\Delta H_1 - \Delta H_0| < C_2\sqrt{\varepsilon}\Delta a.$$

Proof. Since the Hamiltonian takes on different values at the saddles, a tube cannot be $C_1\varepsilon$ -close to both saddles for small enough ε . Also, there exists C_1 such that any tube starting $C_1\varepsilon$ -close to a saddle cannot be $C_1\varepsilon$ -close to the same saddle when it returns to this saddle. This is because this trajectory upon its return near the saddle cannot be in the gray-shaded zone (Figure 13), and by Corollary E.3 the separatrix loop splits by $O(\varepsilon)$ far from the saddle and thus by $O(\sqrt{\varepsilon})$ near the saddle.

Arguing as in the proof of Lemma E.16, we see that it is enough to show that $\iint_{\mathcal{T}} \varepsilon \operatorname{div} \mathbf{f}_{a_0} = O(\Delta a\sqrt{\varepsilon})$. Denote by \mathcal{T}_ε the intersection of \mathcal{T} with the $C_1\varepsilon$ -neighborhood of the saddle. One can show that

$$\iint_{\mathcal{T} \setminus \mathcal{T}_\varepsilon} \varepsilon \operatorname{div} \mathbf{f}_{a_0} = O(\Delta a\sqrt{\varepsilon})$$

as it was done in Lemma E.16. Now let us estimate the same integral over \mathcal{T}_ε . Since $\operatorname{div} \varepsilon \mathbf{f}_{a_0} = \operatorname{div} \mathbf{w}_0$, it is enough to estimate $\iint_{\mathcal{T}_\varepsilon} \operatorname{div} \mathbf{w}_0$. This can be done by applying the divergence theorem to the flux of \mathbf{w}_0 through the beginning of \mathcal{T} bounded by some transversal $R(x)$ close to the boundary of \mathcal{T}_ε (recall that \mathbf{x}_0 is in \mathcal{T}_ε). As the divergence is negative near the saddles, $\iint_{\mathcal{T}_\varepsilon} \operatorname{div} \mathbf{w}_0 < 0$. On the other hand, this integral is the sum of the fluxes through l_0, l_1 , and R . The last of these is positive, so that the absolute value of the integral is bounded by the sum

of the absolute values of the first two terms. The first of these is zero since l_0 is a trajectory of \mathbf{w}_0 . The second term is $O(\Delta a \varepsilon)$ since the flux of \mathbf{w}_1 through l_1 is zero, while $\|\mathbf{w}_1 - \mathbf{w}_0\| = O(\Delta a)$, and the length of l_1 is $O(\varepsilon)$. Thus, the integral over \mathcal{T}_ε is $O(\Delta a \varepsilon)$. \square

Corollary E.19. *There exist $C_1, C_2 > 0$ such that the following holds. If y is such that the trajectory connecting $(-\frac{\pi}{2}, y)$ with $(\frac{\pi}{2}, \hat{P}(y))$ passes $C_1\varepsilon$ -near one of the saddles, then*

$$\frac{\partial}{\partial a} \hat{P} > \frac{L}{b} + O(\sqrt{\varepsilon}) > 0$$

with $|O(\sqrt{\varepsilon})| < C_2\sqrt{\varepsilon}$. Here, $L = x_L + \frac{\pi}{2} = \frac{\pi}{2} - x_R > 0$, where x_L and x_R are the horizontal coordinates of the left and the right saddles, respectively.

Proof. Consider a vertical transversal Γ' and a horizontal transversal Γ shown in Figure 13 that are at the distance $C_\Gamma\varepsilon$ from the saddles, where the constant C_Γ is chosen to be so large that $\frac{\partial H}{\partial x} < 0$ restricted to Γ .¹¹ Let γ denote a trajectory that realizes Poincaré map and passes $O(\varepsilon)$ -close to one of the saddles; such trajectory crosses Γ' or Γ . Consider the tube \mathcal{T} starting at the point of intersection of γ with $\{x = -\pi/2\}$. Consider also an auxiliary tube $\tilde{\mathcal{T}}$ starting at the point $\tilde{\mathbf{x}}_0$ where γ intersects Γ' or Γ . Denote the points where the two trajectories bounding $\tilde{\mathcal{T}}$ cross $\{x = \frac{\pi}{2}\}$ by $\tilde{\mathbf{x}}'_0$ and $\tilde{\mathbf{x}}'_1$. By construction, $\tilde{\mathbf{x}}'_0 = \mathbf{x}'_0$.

First, consider the case when γ passes near the left saddle, in which case it crosses Γ' . For definiteness, suppose $\Delta a > 0$. Since before the crossing γ goes from left to right and $\mathbf{w}_{a_1} - \mathbf{w}_{a_0}$ is close to a constant vector field $(0, \Delta a)$ pointing up, before the transversal crossing l_1 is above l_0 . This means that $y(\mathbf{x}'_1) > y(\tilde{\mathbf{x}}'_1)$, and $y(\mathbf{x}'_1) - y(\mathbf{x}'_0) > y(\tilde{\mathbf{x}}'_1) - y(\tilde{\mathbf{x}}'_0)$. Thus we have (taking into account $\Delta a > 0$) $\frac{\partial}{\partial a} \hat{P}(y) \geq \lim_{\Delta a \rightarrow 0} \frac{y(\tilde{\mathbf{x}}'_1) - y(\tilde{\mathbf{x}}'_0)}{\Delta a}$. By Lemma E.12 we can continue

$$\frac{\partial}{\partial a} \hat{P}(y) \geq \lim_{\Delta a \rightarrow 0} \frac{y(\tilde{\mathbf{x}}'_1) - y(\tilde{\mathbf{x}}'_0)}{\Delta a} \geq -\frac{\pi/2 - (x_s + O(\varepsilon))}{b} + O(|\Delta \tilde{H}_1 - \Delta \tilde{H}_0|/\Delta a),$$

where x_s is the x -coordinate of the left saddle, $x_s \approx -\frac{\pi}{2}$. By Lemma E.18 this gives the required estimate.

Now, suppose that γ passes near the right saddle, thus crossing Γ . For definiteness, suppose $\Delta a > 0$. First, we prove that the intersection of l_1 with Γ is to the left of the intersection of l_0 with Γ . Recall that $\tilde{\mathbf{x}}_0$ and $\tilde{\mathbf{x}}_1$ denote the intersections of l_0 and l_1 , respectively, with Γ . Set $\tilde{\Delta}H_0 = H_0(\tilde{\mathbf{x}}_0) - H_0(\mathbf{x}_0)$ and $\tilde{\Delta}H_1 = H_1(\tilde{\mathbf{x}}_1) - H_1(\mathbf{x}_0)$. Arguing as in Lemma E.16, we get the estimate $\tilde{\Delta}H_1 - \tilde{\Delta}H_0 = O(\sqrt{\varepsilon}\Delta a)$. To compare the two trajectories, we estimate $H_1(\tilde{\mathbf{x}}_1) - H_1(\tilde{\mathbf{x}}_0)$. We have

$$\begin{aligned} H_1(\tilde{\mathbf{x}}_0) &= (H_1 - H_0)(\tilde{\mathbf{x}}_0) + H_0(\tilde{\mathbf{x}}_0) = (H_1 - H_0)(\tilde{\mathbf{x}}_0) + H_0(\mathbf{x}_0) + \tilde{\Delta}H_0 = \\ &= (H_1 - H_0)(\tilde{\mathbf{x}}_0) - (H_1 - H_0)(\mathbf{x}_0) + H_1(\mathbf{x}_0) + \tilde{\Delta}H_0 = \\ &= -\Delta a(x(\tilde{\mathbf{x}}_0) - x(\mathbf{x}_0)) + (\tilde{\Delta}H_0 - \tilde{\Delta}H_1) + H_1(\tilde{\mathbf{x}}_1). \end{aligned}$$

This gives $H_1(\tilde{\mathbf{x}}_1) = H_1(\tilde{\mathbf{x}}_0) + \Delta a(x(\tilde{\mathbf{x}}_0) - x(\mathbf{x}_0)) + O(\sqrt{\varepsilon}\Delta a) > H_1(\tilde{\mathbf{x}}_0)$. Recall that by our choice of the transversals we have $\frac{\partial H_1}{\partial x} < 0$ on Γ . This implies $x(\tilde{\mathbf{x}}_1) < x(\tilde{\mathbf{x}}_0)$.

Now, we can argue as in the first case considering auxiliary tube $\tilde{\mathcal{T}}$ starting at $\tilde{\mathbf{x}}_0$. This gives (using x_s for the x -coordinate of the right saddle)

$$\begin{aligned} \frac{\partial}{\partial a} \hat{P}(y) &\geq \lim_{\Delta a \rightarrow 0} \frac{y(\tilde{\mathbf{x}}'_1) - y(\tilde{\mathbf{x}}'_0)}{\Delta a} \geq -\frac{\pi/2 - (x_s + O(\varepsilon))}{b} + O(|\Delta \tilde{H}_1 - \Delta \tilde{H}_0|/\Delta a) \geq \\ &\geq \frac{L}{b} + O(\sqrt{\varepsilon}). \end{aligned}$$

\square

¹¹This can be done as $-\frac{\partial H}{\partial x}$ is the vertical component of the Hamiltonian vector field $\mathbf{v} = (\mathbf{v} + \varepsilon \mathbf{f}) + O(\varepsilon)$, and the vertical component of $\mathbf{v} + \varepsilon \mathbf{f}$ is positive and larger than $0.01C_\Gamma\varepsilon$ because Γ is below the saddle.

Proof of Lemma 5.3. Together, Corollaries E.17 and E.19 imply that $\frac{\partial}{\partial a} \hat{P}(y) > 0$ for any y such that the Poincaré map is defined. In Lemma 5.3 the Poincaré map \tilde{P} was written using the coordinate $z = \frac{y-x}{2\pi}$, and we have $\frac{\partial}{\partial a} \tilde{P}(y) = \frac{1}{2\pi} \frac{\partial}{\partial a} \hat{P}(y) > 0$. \square

References

- [1] Martin R Maxey and James J Riley. “Equation of motion for a small rigid sphere in a nonuniform flow”. In: *The Physics of Fluids* 26.4 (1983), pp. 883–889.
- [2] J.P. Gollub T. Sapsis N.T. Ouellette and G. Haller. “Neutrally buoyant particle dynamics in fluid flows: Comparison of experiments with Lagrangian stochastic models”. In: *Physics of Fluids* 23 (2014), pp. 093304-1-093304–15.
- [3] M. Farazmand G.P. Langlois and G. Haller. “Asymptotic dynamics of inertial particles with memory”. In: *arXiv:1409.0634v1* (2014), pp. 1–24.
- [4] Jorge Arrieta, Ana Barreira, and Idan Tuval. “Microscale patches of nonmotile phytoplankton”. In: *Physical review letters* 114.12 (2015), p. 128102.
- [5] AW Baggaley. “Stability of model flocks in a vortical flow”. In: *Physical Review E* 93.6 (2016), p. 063109.
- [6] Hannah Kreczak, Rosie Higgins, and Andrew J Willmott. “The Dynamics of Buoyant Microplastic in the Ocean Forced by Unsteady Insolation”. In: *Journal of Marine Science and Engineering* 11.7 (2023), p. 1402.
- [7] MR Maxey and S Corrsin. “Gravitational settling of aerosol particles in randomly oriented cellular flow fields”. In: *Journal of the atmospheric sciences* 43.11 (1986), pp. 1112–1134.
- [8] A Sarracino, F Cecconi, A Puglisi, and Angelo Vulpiani. “Nonlinear response of inertial tracers in steady laminar flows: differential and absolute negative mobility”. In: *Physical review letters* 117.17 (2016), p. 174501.
- [9] F Cecconi, A Puglisi, A Sarracino, and A Vulpiani. “Anomalous force-velocity relation of driven inertial tracers in steady laminar flows”. In: *The European Physical Journal E* 40 (2017), pp. 1–5.
- [10] Antoine Renaud and Jacques Vanneste. “Dispersion of inertial particles in cellular flows in the small-Stokes, large-Péclet regime”. In: *Journal of Fluid Mechanics* 903 (2020), A2.
- [11] Anu VS Nath, Anubhab Roy, Rama Govindarajan, and Sivaramakrishnan Ravichandran. “Transport of condensing droplets in Taylor-Green vortex flow in the presence of thermal noise”. In: *Physical Review E* 105.3 (2022), p. 035101.
- [12] H Shin and MR Maxey. “Chaotic motion of nonspherical particles settling in a cellular flow field”. In: *Physical Review E* 56.5 (1997), p. 5431.
- [13] MF Piva and S Gabbanelli. “A single dumbbell falling under gravity in a cellular flow field”. In: *Journal of Physics A: Mathematical and General* 36.15 (2003), p. 4291.
- [14] Colin Torney and Zoltán Neufeld. “Transport and aggregation of self-propelled particles in fluid flows”. In: *Physical review letters* 99.7 (2007), p. 078101.
- [15] Qingqing Yin, Jianli Liu, Yunyun Li, and Fabio Marchesoni. “Diffusion of noiseless active particles in a planar convection array”. In: *Physical Review E* 109.6 (2024), p. 064211.
- [16] J Ravnik, M Hribersek, F Vogel, and P Steinmann. “Numerical simulation of particle movement in cellular flows under the influence of magnetic forces”. In: *International journal of simulation modelling* 13.3 (2014), pp. 300–311.
- [17] Jimmy Chi Hung Fung. “Gravitational settling of small spherical particles in unsteady cellular flow fields”. In: *Journal of aerosol science* 28.5 (1997), pp. 753–787.
- [18] CC Chan and Jimmy Chi Hung Fung. “The change in settling velocity of inertial particles in cellular flow”. In: *Fluid dynamics research* 25.5 (1999), p. 257.
- [19] Claudia Venditti, Massimiliano Giona, and Alessandra Adrover. “Invariant manifold approach for quantifying the dynamics of highly inertial particles in steady and time-periodic incompressible flows”. In: *Chaos: An Interdisciplinary Journal of Nonlinear Science* 32.2 (2022).

- [20] H Stommel. “Trajectories of small bodies sinking slowly through convection cells”. In: *Journal of Marine Research* 8 (1949), pp. 24–29.
- [21] J Rubin, CKRT Jones, and M Maxey. “Settling and asymptotic motion of aerosol particles in a cellular flow field”. In: *Journal of Nonlinear Science* 5 (1995), pp. 337–358.
- [22] MR Maxey. “The motion of small spherical particles in a cellular flow field”. In: *The Physics of fluids* 30.7 (1987), pp. 1915–1928.
- [23] Lian-Ping Wang, MR Maxey, TD Burton, and DE Stock. “Chaotic dynamics of particle dispersion in fluids”. In: *Physics of Fluids A: Fluid Dynamics* 4.8 (1992), pp. 1789–1804.
- [24] Martin R Maxey and Gelonia L Dent. “Modeling and simulation of discrete particles in fluid flow”. In: *Collective Dynamics of Particles: From Viscous to Turbulent Flows* (2017), pp. 1–38.
- [25] Sergei Petrovich Novikov. “The Hamiltonian formalism and a many-valued analogue of Morse theory”. In: *Russian mathematical surveys* 37.5 (1982), p. 1.
- [26] VI Arnold. “Topological and ergodic properties of closed 1-forms with incommensurable periods”. In: *Func. Anal. Appl* 25 (1991), pp. 81–90.
- [27] A. Zorich V.I. Arnold M. Kontsevich. “Pseudoperiodic topology”. In: American Mathematical Soc., 1999. Chap. How do the leaves of a closed 1-form wind around a surface?
- [28] IA Dynnikov, A Ya Maltsev, and SP Novikov. “Chaotic Trajectories on Fermi Surfaces and Nontrivial Modes of Behavior of Magnetic Conductivity”. In: *Journal of Experimental and Theoretical Physics* 135.2 (2022), pp. 240–254.
- [29] Vladimir I Arnold. “Small denominators. I. Mapping the circle onto itself”. In: *Izv. Akad. Nauk SSSR Ser. Mat* 25.1 (1961), pp. 21–86.
- [30] Robert E Ecke, J Doyne Farmer, and David K Umberger. “Scaling of the Arnold tongues”. In: *Nonlinearity* 2.2 (1989), p. 175.
- [31] Colin Boyd. “On the structure of the family of Cherry fields on the torus”. In: *Ergodic Theory and Dynamical Systems* 5.1 (1985), pp. 27–46.
- [32] Grzegorz Świątek. “Endpoints of rotation intervals for maps of the circle”. In: *Ergodic Theory and Dynamical Systems* 9.1 (1989), pp. 173–190.
- [33] JJP Veerman. “Irrational rotation numbers”. In: *Nonlinearity* 2.3 (1989), p. 419.
- [34] J Graczyk, G Świątek, FM Tangerman, and JJP Veerman. “Scalings in Circle Maps III”. In: *arXiv preprint math/9202209* (2017).
- [35] Liviana Palmisano and Bertuel Tangué Ndawa. “A phase transition for circle maps with a flat spot and different critical exponents”. In: *Discrete and Continuous Dynamical Systems* 41.11 (2021), pp. 5037–5055.
- [36] Philip Boyland. “On the abundance of k-fold semi-monotone minimal sets in bimodal circle maps”. In: *Ergodic Theory and Dynamical Systems* 44.5 (2024), pp. 1269–1314.
- [37] IA Dynnikov. “Semiclassical motion of the electron. A proof of the Novikov conjecture in general position and counterexamples”. In: *Translations of the American Mathematical Society-Series 2* 179 (1997), pp. 45–74.
- [38] Bassam Fayad, Adam Kanigowski, and Rigoberto Zelada. “A non-mixing Arnold flow on a surface”. In: *arXiv preprint arXiv:2308.01247* (2023).
- [39] George Haller and Themistoklis Sapsis. “Where do inertial particles go in fluid flows?” In: *Physica D: Nonlinear Phenomena* 237.5 (2008), pp. 573–583.
- [40] N. Fenichel. “Persistence and Smoothness of Invariant Manifolds for Flows”. In: *Indiana University Mathematics Journal* 21.3 (1971), pp. 193–226.
- [41] Christopher KRT Jones. “Geometric singular perturbation theory”. In: *Dynamical Systems: Lectures Given at the 2nd Session of the Centro Internazionale Matematico Estivo (CIME) held in Montecatini Terme, Italy, June 13–22, 1994* (1995), pp. 44–118.

- [42] George Pólya and Gabor Szegő. *Problems and theorems in analysis II: theory of functions. Zeros. Polynomials. Determinants. Number theory. Geometry.* Springer Science & Business Media, 2012.
- [43] J Jr Palis and Welington De Melo. *Geometric theory of dynamical systems: an introduction.* Springer Science & Business Media, 2012.
- [44] Vladimir I Arnold. *Ordinary differential equations.* Springer Science & Business Media, 1992.

Mark Levi,
Department of Mathematics,
Pennsylvania State University,
University Park, State College, PA 16802
E-mail : mxl48@psu.edu

Alexey Okunev,
Department of Mathematics,
Pennsylvania State University,
University Park, State College, PA 16802
E-mail : abo5297@psu.edu